Preface

Novel and significant changes in the area of oncologic imaging have had a positive impact on the ability to non-invasively stage bladder, prostate, penile, testicular, adrenal, and renal tumors. Most of these imaging enhancements are closely related and parallel the clinical impact of these tumors: for example as prostate cancer becomes the most common malignancy in men, there is a push to use imaging for both accurate staging prior to therapy and also as a means to follow patients after therapy. Most of the novel and cutting-edge therapeutic techniques being developed to treat these genitourinary tumors are increasingly more dependent on imaging for better tumor delineation and evaluation. The mainstay for imaging used to be conventional imaging techniques with transrectal and transabdominal ultrasound, angiography, and intravenous contrast studies. Significant improvements in image processing and resolution in cross-sectional imaging with computed tomography, magnetic resonance imaging, and now single photon emission computed tomography have brought dramatic changes in our ability to assess genitourinary malignancies of all types. Improvements in contrast agents and superimposition of functional studies with anatomical studies have now made molecular imaging with radionuclides part of our armamentarium for these neoplasms.

What can the expected impact of imaging be on the future of uro-oncology? Although the current orientation for imaging has been anatomic and organ specific, the striking improvements in imaging related to functional activity are now being combined with the anatomic data to give a more complete assessment of the disease process in all stages. The development of new molecular markers and the incorporation of virtual technology will provide a true fusion of technology that is bound to have an impact on our management of oncological problems. We are currently limited by our inability to detect disease at its earliest stages, follow it closely through a course of therapy, and monitor it after treatment. Imaging is a major key to improvements that may make management of cancer similar to that of other chronic diseases such as diabetes or hypertension. This text presents the state of the art for imaging in urological oncology and gives a glimpse of future directions for research in this exciting field.

Jean de la Rosette
Michael Manyak
Mukesh Harisinghani
Hessel Wijkstra

Chapter 11

Urothelial Cell Carcinoma of the Upper Urinary Tract: Introduction

B.A. Inman, M.L. Blute, and R.P. Hartman

Introduction

Urothelium is the specialized epithelium that covers the urinary collecting system from the tips of the renal papillae to the prostatic urethra. Tumors of the urothelium can be benign but the vast majority are malignant carcinomas. Carcinomas of the urothelium are common and the upper urinary tract is the affected site in roughly 5% of cases. Similarly, 5–10% of tumors that involve the kidney actually arise from the renal collecting system. It is unusual to find an upper urinary tract tumor as a result of screening imaging. Rather, most patients present with symptoms of flank pain or hematuria and are evaluated specifically to rule out tumoral involvement of the collecting system. Nonetheless, a thorough evaluation of the collecting systems should be routinely sought in most renal imaging procedures, even if typical symptoms are not present.

This chapter discusses widely available imaging modalities used to diagnose upper urinary tract tumors: ultrasonography, intravenous pyelography, retrograde pyelography, and antegrade pyelography. For each of these imaging techniques we have attempted to present a discussion of special indications for usage, practical strengths and weaknesses, interpretation pointers and pitfalls, evidence of efficacy for diagnosing upper urinary tract tumors, and potential complications resulting from usage. References are used liberally and are meant to provide a comprehensive reading list for the reader interested in further exploring the published evidence for the imaging modalities and ideas presented herein.

B.A. Inman (✉)
Assistant Professor of Urology, DUMC 2812
Duke University Medical Center, Durham, NC 27710
e-mail: brant.inman@duke.edu

Ultrasonography

The Normal Upper Urinary Tract

Kidney

Ultrasound examination of the kidney is typically performed with a 2.5–5 MHz transducer with the patient in any one of a number of positions. The kidneys are usually best viewed on deep inspiration and transverse and longitudinal images are obtained. Characteristics that should be routinely examined are the size and shape of the kidney, the echogenicity of the cortex relative to the spleen and liver, the thickness of the cortex, the degree of corticomedullary differentiation, and the structure of the intrarenal collecting system (i.e., calyces and renal pelvis).

The kidney usually has a smooth contour that resembles a bean although persistent fetal lobulation is a common normal variant. The spleen or liver may indent the upper pole of the kidney giving the impression of a dromedary hump. The adult renal cortex is thickest at the poles of the kidney where it is approximately 15 mm thick [1]. The renal medulla is principally comprised of 10–12 triangular renal pyramids that contain the collecting ducts and loops of Henle of the nephron. The pyramids are hypoechoic relative to the cortex and are separated from one another by fingers of interpyramidal renal cortex called the columns of Bertin. The rounded apex of each renal pyramid—called the papilla—projects into a minor calyx where it drains the urine flowing through its collecting ducts.

Renal Calyces and Pelvis

The 10–12 minor calyces then drain into 2–3 major calyces which coalesce to form the renal pelvis. The renal pelvis can assume a wide variety of normal shapes and may not be symmetric with the contralateral side. This pleomorphism can make diagnosing obstruction difficult at times. The renal

J.J.M.C.H. de la Rosette et al. (eds.), *Imaging in Oncological Urology*,
DOI 10.1007/978-1-84628-759-6_11,

calyces and pelvis are located in a central concavity in the kidney that is called the renal sinus. Fatty tissue is abundant in the renal sinus of adults and accounts for its hyperechogenic appearance on ultrasound [2]. In renal ultrasonography, the normal order of increasing tissue echogenicity is renal medulla, renal cortex, liver and spleen, pancreas, and renal sinus. Demonstration of the urothelium that lines all the collecting system is not always possible but, when it is visible, it should appear as a slightly hyperechogenic layer that is smooth, thin, and regular. The renal pelvis and calyces drain into the same retroperitoneal lymph nodes as the kidney: the left side drains primarily into the para-aortic, preaortic, and postaortic nodes while the right side drains principally into the paracaval and interaortocaval nodes.

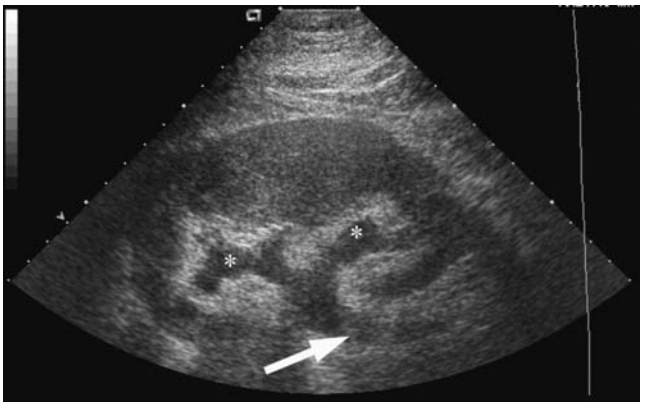

Fig. 11.1 Longitudinal ultrasound image of the left kidney demonstrates dilatation of the intrarenal collecting system (*asterisk*) with a dilated proximal ureter (*arrow*)

Ureter

Drainage of the renal pelvis into the ureter occurs at the ureteropelvic junction, a common site for both congenital and acquired obstructions. The ureter courses in the retroperitoneal space on top of the psoas muscle and is situated lateral to the vertebral pedicles until it deviates medially and crosses the common iliac artery (at the level of its bifurcation) to enter the pelvis. The retroperitoneal ureters should be at least 5 cm apart and should have a slight S shape. The pelvic portion of the ureter enters the trigone of the bladder posteriorly after passing in close proximity to the uterine artery and cervix in the female. Ureteral length varies with age, gender, and height but averages around 24 cm. Normal ureters are not routinely seen with ultrasonography but dilated ureters are. The lymphatic drainage of the ureters follows a course similar to the ureteral vasculature. The retroperitoneal portion of the left ureter drains medially into the para-aortic and presacral nodes whereas the right retroperitoneal ureter drains medially into the paracaval and interaortocaval nodes. Both pelvic ureters drain laterally into the internal iliac, external iliac, and common iliac nodes.

Upper Urinary Tract Obstruction

Renal ultrasonography (RUS) may be the first imaging modality used to investigate a patient with flank pain or hematuria, both of which may be presenting signs of an upper urinary tract tumor [3, 4]. The most frequent complication of an upper urinary tract tumor that can be seen with RUS imaging is urinary tract obstruction leading to *collecting system dilation* (Fig. 11.1). Though early account of RUS described an impressive sensitivity of 98% for diagnosing obstruction, the specificity was only 74% [5]. It was quickly recognized that the cause of the high false-positive rate was a number of non-obstructive entities that produce a dilation of the collecting system that can closely mimic obstruction [6]. Technological advances in ultrasonography have helped to reverse these early problems of diagnostic accuracy and the combination of higher ultrasound frequencies, better transducers, and better software has resulted in dramatically improved image resolution. The single most important development in renal ultrasound in the last 20 years, however, has been the acquisition of the capability to perform Doppler flow analysis [7]. The expansion of early Doppler technology has led to the clinical applications of waveform Doppler sonography, power Doppler sonography, and color Doppler sonography. This, in turn, has allowed the ultrasonographer to measure the *renal resistive index* and *ureteral jets* (Fig. 11.2) [8–10], both of which can help to diagnose veritable renal obstruction.

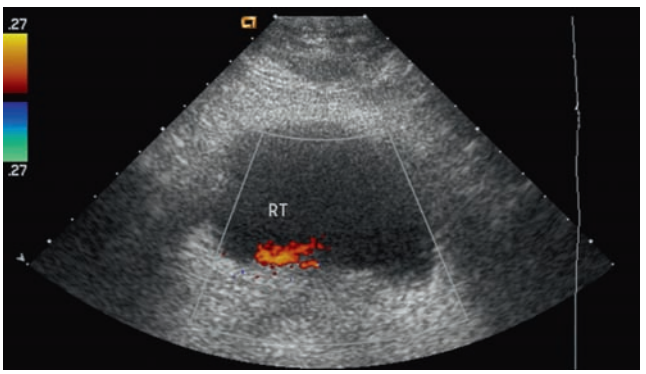

Fig. 11.2 Transverse Doppler ultrasound image of the bladder demonstrates a normal right ureteral jet. The left ureteral jet is absent suggestive of left sided obstruction

Renal Pelvic Tumors

If large enough, urothelial tumors of the renal pelvis can be visualized directly by ultrasound. Although finding a mass in the renal collecting system can sometimes be very difficult with ultrasound, an equally important task is ruling out a number of non-malignant pathologies that can cause a mass lesion in the renal pelvis (Table 11.1). A recent manuscript provides an excellent review of the diagnostic imaging features of lesions of the renal sinus [11].

Separation of the Central Echo Complex

Renal pelvic tumors can cause separation of the normally echodense central renal sinus if they are large enough [2, 12, 13]. The appearance of separation of the central echo seen in upper tract tumors is similar to what is seen in hydronephrosis but can be distinguished from the former by the presence of residual echoes and the absence of the acoustic enhancement (Fig. 11.3) [12]. The presence of a central renal mass of moderate echogenicity that is separated from the renal parenchyma by a rim of highly echogenic renal sinus fat should be considered a malignant urothelial tumor until proven otherwise [2, 13].

Table 11.1 Differential diagnosis for a collecting system filling defect

Calculi
Calyceal papilla
Cancer
Clots
Contrast air bubble
Cyclical endometriosis
Contamination/cultures
Fungus ball (mycetoma)
Schistosomiasis
Tuberculosis
Chronic inflammation
Cystic ureteropyelitis
Malakoplakia
Leukoplakia/cholesteatoma
Congenital
Vascular imprint
Kinks

Fig. 11.3 Longitudinal ultrasound image of the right kidney demonstrates soft tissue with similar echogenicity as the renal parenchyma (*asterisk*) separating the normal renal sinus fat. The findings are due to a large TCC in the upper pole of the kidney

Echogenicity

Urothelial tumors tend to have an echogenicity that is similar to the renal cortex but less than the normal renal sinus [12, 13]. Blood clots can have varying degrees of echogenicity and may be quite difficult to differentiate from a tumor [14, 15]. Renal calculi tend to be more echogenic than tumors and, due to their high density, calculi usually demonstrate acoustic shadowing (the cone-dome) characteristic of calcium deposition [15–18]. Calcification may also be present in tuberculous and schistosomal infection of the urinary tract [19–25]. However, it should be kept in mind that rare urothelial tumors may present with intratumoral calcification in a pattern that has been described as coarse and punctate [26]. Furthermore, certain upper urinary tract tumors—particularly squamous cell carcinomas—arise in the context of chronic irritative renal urolithiasis [27–31]. One group has even reported acoustic shadowing in a tumor [32]. Therefore, though the presence of calcification, a renal pelvic stone, or acoustic shadowing does not absolutely rule out a renal pelvic tumor, it certainly does suggest alternate diagnoses.

Mobility

One feature that can distinguish a urothelial tumor from other potential intraluminal masses is its lack of mobility. While necrotic papillae, blood clots, and certain calculi may move with a change in patient position, tumors are fixed to the urothelium and should not move [12].

Contour

Though by no means absolute, urothelial tumors of the renal pelvis tend to be poorly defined and have irregular contours while blood clots and stones tend to have sharp smooth contours [12]. Considerable overlap exists, however, and stones can be ragged and tumors smooth. Another problem is that contours are difficult to assess with ultrasonography. For these reasons contours are often of little use in diagnosing urothelial tumors by ultrasonography [33].

Blood Flow

The demonstration of blood flow within a urothelial mass is pathognomonic for a neoplastic process [33–38]. Of the few reported upper tract urothelial carcinomas that have been evaluated by Doppler ultrasonography, most have shown a Doppler shift greater than 2 kHz [34, 35].

Large Tumors

Large tumors of the central kidney that are clearly invading both the collecting system and the renal parenchyma are nearly impossible to categorize with certainty using ultrasonography [39]. These lesions can represent a renal tubular neoplasm that has invaded the collecting system or a urothelial neoplasm that has grown into the renal parenchyma. CT scanning may perform better than ultrasonography in this setting but is by no means a perfect technique [40, 41]. If treatment decisions are to be influenced by the histologic tumor type, a pretreatment biopsy should be considered.

Ureteral Tumors

Ultrasonography has not been traditionally considered a good way to assess for ureteral tumors. Whereas other imaging modalities can show a variety of imaging findings in cases of ureteral tumors, ultrasonography typically demonstrates two things: a ureteral mass or its associated hydronephrosis [37, 42, 43]. Ureteral tumors have similar features to the renal pelvic tumors described earlier in that they are of moderate echogenicity, show no acoustic shadowing, and are rarely calcified. Evidence of Doppler flow in a ureteral mass is likewise considered pathognomonic for tumor [38]. Comparative studies of the various imaging modalities for ureteral tumors are rare but at least one group has shown ultrasonography to be superior to CT in detecting these uncommon tumors [42].

Advantages of Ultrasonography

Ultrasonography is probably not the best overall method for evaluating the upper urinary tract for cancer. Nonetheless, it does have certain advantages that deserve special mention.

Noninvasive

Unlike all other methods of evaluating the upper urinary tract, ultrasonography does not require intravenous access, a percutaneous nephrostomy, or a ureteral catheter. The risk of iatrogenic injury to the body is therefore practically nonexistent.

No Contrast

All other forms of urography require the administration of potentially toxic and allergenic contrast agents. Contrast-associated side effects are not a minor problem and will be discussed in more detail in the section Intravenous Pyelography.

Renal Insufficiency

Patients with impaired renal function are at high risk for contrast nephrotoxicity and should generally be spared contrast if possible. If the kidney is non-functional because of severe tumoral obstruction or some other process, contrast excretion will be markedly impaired and the quality of the imaging will suffer dramatically. Ultrasonography can be used safely and effectively in patients with renal failure.

Radiation

Ultrasonography does not use ionizing radiation to image the body and is generally considered to be free of significant side effects [44]. This important fact makes it the ideal imaging study for pregnant women. It should also be remembered that imaging-related neoplasia is a possibility for diagnostic imaging modalities that use ionizing radiation [45–48]. This may be particularly relevant for cancer patients who undergo repeated imaging tests.

Cost

Along with IVP, ultrasonography is probably the most inexpensive diagnostic test for evaluating the upper urinary tract.

Disadvantages of Ultrasonography

Calculi

Ultrasonography is not very sensitive for diagnosing renal calculi [49–52]. Since most patients with upper tract tumors are initially evaluated for flank pain or hematuria and stones are a much more common cause of these symptoms than urothelial tumors, the initial evaluation of flank pain and

hematuria should employ a technique that is very sensitive for detecting stones (such as noncontrast CT) [53–55].

Staging

If a urothelial tumor is detected on initial imaging, staging the tumor then becomes a very important consideration. Conventional ultrasonography is inferior to CT and MRI for detecting retroperitoneal and pelvic lymph node enlargement [56–60], for detecting hepatic metastases [61–63], and for evaluating the lungs [64–66]. There is one particular advantage to ultrasonography for tumor staging, however: evaluation of the renal vein. Like renal cell carcinomas, urothelial carcinomas can invade the renal vein and spread to the inferior vena cava, albeit much less frequently [67]. Color Doppler imaging may be more accurate than CT in identifying tumor thrombus in the renal vein or vena cava [68–71].

Operator Dependence

Ultrasonography is operator dependent: the better the ultrasonographer, the better the accuracy [72–76]. Cross-sectional imaging modalities appear to have better interobserver reproducibility than ultrasonography.

New Advances in Ultrasonography

Endoluminal Ultrasonography

The use of intraureteral ultrasonography was first reported in the 1990s and the first report of the diagnosis of ureteral tumor occurred shortly thereafter [77, 78]. Endoluminal ultrasonography has not been widely adopted in the 15 years since it was introduced despite the refinement of smaller and more accurate probes. Its use has been principally limited to the diagnosis of crossing vessels at the ureteropelvic junction in a few select medical centers [79–83]. There have been just a few reports of its employment in diagnosing urothelial tumors of the ureter and renal pelvis [77, 84, 85]. The authors of these studies cite the principle benefit of better preoperative staging of the tumor due to more accurate identification of the ureteral mucosa and musculature. This staging advantage would only benefit the minority of patients with upper tract tumors that are considering endoscopic management. Newer modifications of the technique involve 3D reconstruction of the upper urinary tract [86, 87].

Microbubble Contrast Agents

One of the most exciting advances in ultrasonography has been the development of the technique of contrast-enhanced ultrasonography that has the potential to greatly improve diagnostic accuracy [88, 89]. The contrast agents that have been developed for ultrasound consist principally of small air bubbles measuring 3 μm in diameter that can be injected into the bloodstream or the urinary tract. At high ultrasound frequencies these microbubbles are over a thousand times more echogenic than the surrounding normal tissues [90]. Applications that are relevant to urothelial tumors include improved visualization of liver metastases [91, 92], improved imaging of tumor microvascularity [93], retrograde imaging of the ureter without radiation [94–96], molecular imaging [97], and the delivery of drugs to specific targets [88].

Intravenous Pyelography (IVP)

Brief History

After the development of medical X-rays by Roentgen in 1895, the first step toward the development of intravenous pyelogram was the development of radiocontrast. Radiocontrast was first used to visualize the urinary collecting in the form of retrograde pyelography (see discussion below) [98]. Early contrast agents—such as colloidal silver, thorium, and colloidal silver iodide—were toxic irritants that harmed the urinary tract and occasionally resulted in patient deaths. A major advance occurred in 1918 when Donald Cameron from the University of Minnesota introduced sodium iodide as a new contrast agent [99]. This agent was remarkable because it was much less toxic than other contrast agents available at the time. Mayo Clinic physicians Earl Osborne (Fig. 11.4), Charles Sutherland, Albert Scholl, and Leonard Rowntree (Fig. 11.5) used intravenous sodium iodide to produce the first intravenous pyelogram in 1918 and reported the results of their initial series in 1923 [100]. The result was a revolution in medical imaging and the next 75 years were spent trying to find contrast agents with better imaging characteristics and lower toxicity. German physician Leopold Lichtwitz was key to the development of novel contrast agents. He recruited American physician Moses Swick to a fellowship position in his laboratory in Hamburg, and the young American physician began screening multiple new agents as potential contrast agents. Swick soon moved to Berlin and began working with Alexander von Lichtenberg, the discoverer of the retrograde pyelogram, on newer and better agents. They teamed up with Arthur Binz, a Berlin chemist that had provided chemicals to Swick while he was in Hamburg,

Fig. 11.4 Earl Osborne, Mayo Clinic dermatology resident, 1918–1923

Fig. 11.5 Leonard Rowntree, Mayo Clinic internist, 1920–1932

and eventually the ionic compound Uroselectan (Iopax) was developed [101]. Uroselectan was eventually replaced by ionic monomers (e.g., diatrizoate, iothalamate) then by triiodinated nonionic compounds (e.g., iohexol/Omnipaque), and finally by iso-osmolar nonionic compounds (e.g., iodixans/Visipaque). With these newer agents, IVP has become a safer and better diagnostic test.

More recently, questions have surfaced as to whether IVP is dead, dying or neither [102–106]. Though IVP may no longer be the primary diagnostic modality for evaluating the urinary tract, we argue that it certainly has its place in current practice. CT and MR urography simply do not demonstrate the anatomic detail of the renal pelvis and ureter that IVP and retrograde pyelography offer [107]. These techniques are still useful and need not be abandoned.

Technique

Patient preparation is not routinely required for IVP but certain key points should be observed. Patients should be well hydrated and have adequate renal function (see section Disadvantages of IVP) and an empty bladder. The following film sequences are a suggestion for a typical case but it should be recalled that IVP should be tailored to each clinical circumstance [108]. A summary of the IVP procedure that we use at the Mayo Clinic has been previously published [109]. A scout film is first obtained and is followed by 300–600 mg/kg of contrast medium injected as a bolus into the bloodstream. An initial film coned to the kidneys can be obtained at 1 minute to demonstrate the nephrogram. A second film is obtained at 5 minutes to assess the progress of opacification of the parenchyma and collecting system. This film should include the inferior margin of the symphisis pubis and the suprarenal region. A third film is obtained at 10 minutes to view the collecting system which should be filled with contrast by this point in time. Visualization of the collecting system on this film can be improved by abdominal compression or by Trendelenberg positioning (Fig. 11.6). We routinely commence our abdominal compression shortly after contrast injection and center it at the iliac crest where the ureters can be compressed against the bony pelvis. If the collecting system is not seen perfectly, oblique films may be of use. It is recommended that at least two images of any collecting system defect be obtained. A fourth film of the ureters and full bladder can be obtained at 10–15 minutes (after release of abdominal compression) followed by a fifth post-micturition film. If there is evidence of obstruction and the collecting system has not filled adequately, delayed films should be sought.

Fig. 11.6 Image from an intravenous pyelogram demonstrates a TCC in a lower pole infundibulum of the right kidney (*arrow*). External compression, as in this case, is useful for optimal distension of the intrarenal collecting system

Fig. 11.7 Image from an intravenous pyelogram demonstrates left renal enlargement, dilation of the left renal collecting system and absence of filling of the left ureter

Imaging Features

Calcification

Calcification in upper tract tumors and their mimics is discussed in section Renal Pelvic Tumors. Calcification is sought on the scout film and its position confirmed following contrast injection.

Delayed Nephrogram

When the collecting system of one of two kidneys is obstructed, compensatory hemodynamic changes lead to a reduction in its glomerular filtration rate predominantly through afferent arteriolar vasoconstriction [110–114]. The reduced renal blood flow delays the passage of radiocontrast from the renal artery to the nephron and the imaging result is a delay in the nephrogram. The delay is usually best appreciated by comparing the normal unobstructed kidney to the obstructed kidney. It is noteworthy that renal units that are obstructed bilaterally or that are solitary and obstructed may not show this imaging feature because they undergo a different series of hemodynamic responses to obstruction [113].

Increased Renal Size

Obstruction of the renal collecting system usually (but not always) results in progressive dilation of the ureter and renal pelvis. The dilated kidney appears larger during the nephrographic phase of the IVP (Fig. 11.7).

Distortion of the Renal Contour

The interpapillary line is the curved line that joins the tips of the minor calyces [108]. A change in parenchymal thickness can be appreciated by comparing the distance from the interpapillary line to the edge of the renal parenchyma visualized on the nephrogram of the kidney. When the parenchyma is thickened and the underlying collecting system is abnormal, a renal mass lesion should be suspected. Renal masses can also produce a double contour that is best appreciated at tomography. Parenchymal beaking occurs when there is thickening of the parenchyma at the margins of an intraparenchymal renal lesion and indicates the presence of a slow-growing mass. Non-enhancing parenchymal thickening is typical of a renal cyst.

Fig. 11.8 Image from an intravenous pyelogram 45 minutes after injection demonstrates a dilated right intrarenal collecting system and upper ureter (*arrow*). There is persistence of the right nephrogram relative to the left. These secondary findings of obstruction were due to a distal right ureteral TCC (not shown)

Fig. 11.9 Image from an intravenous pyelogram demonstrates an amputated calyx in the upper pole of the right kidney (*arrow*). This was shown to be due to an obstructing TCC in the upper pole infundibulum

Pyelocaliectasis

Dilation and distortion of the calyces and renal pelvis are usually signs of obstruction though there are many other pathologies that can affect the collecting system anatomy (Fig. 11.8). Pathologies that should be considered include infection and post-infectious scarring (particularly tuberculosis, fungal infections, and schistosomiasis) [19, 24, 115], papillary necrosis [116–119], calyceal diverticulae [120, 121], and infundibular stenosis. Papillary necrosis can be diagnosed by carefully evaluating the minor calyces for a series of suggestive signs while infections are ruled out by urinalysis and urine cultures.

Phantom Calyx

A phantom calyx (a.k.a. aborted calyx) is a calyx that does not fill with contrast on imaging (Fig. 11.9) [122]. It is thought that phantom calyces generally represent serious pathology in the kidney and the differential diagnosis includes tuberculosis, urolithiasis, neoplasia (usually originating from nephron or urothelium), and congenital malformation. A tumor-filled calyx that is non-visualized has been termed an oncocalyx [108].

Filling Defects

Filling defects are likely the most common imaging feature of urothelial tumors of the renal pelvis and may be the second most common feature of ureteral tumors (after hydronephrosis) (Fig. 11.10) [18, 123–126]. The differential

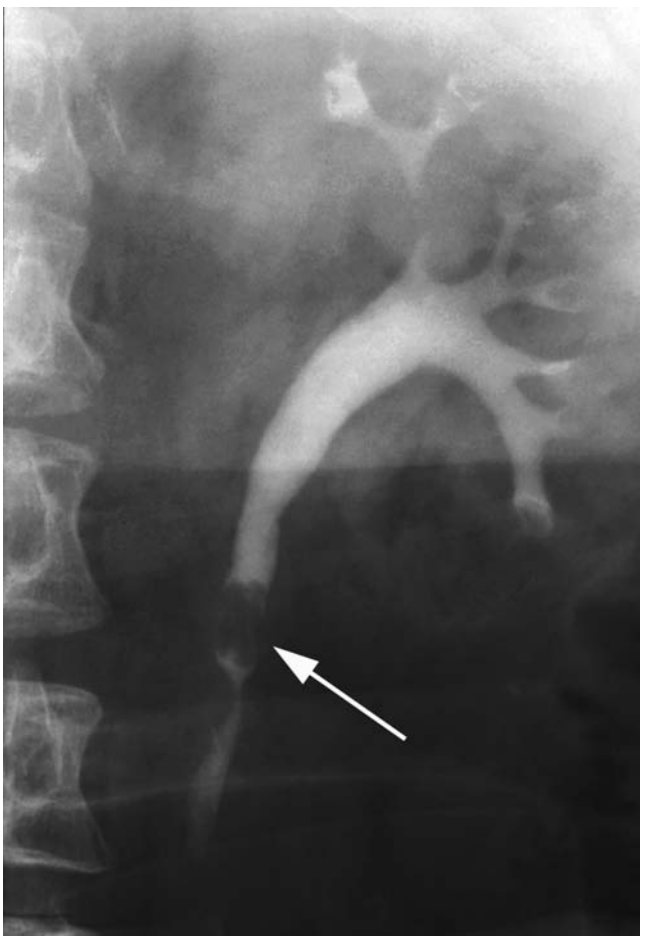

Fig. 11.10 Image from an intravenous pyelogram demonstrates a TCC in the upper left ureter (*arrow*)

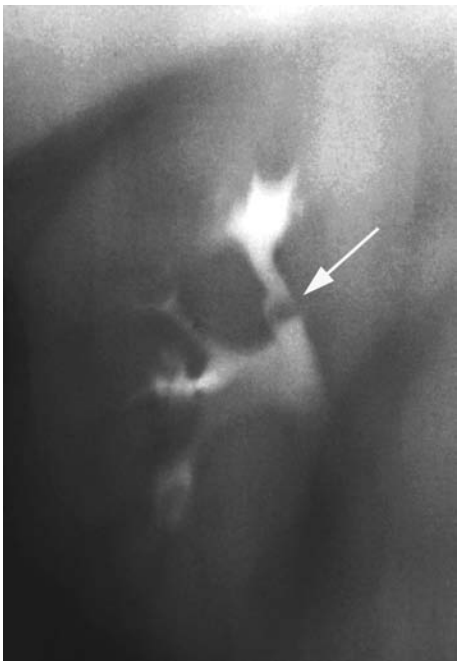

Fig. 11.11 Tomographic image from an intravenous pyelogram demonstrates a tiny TCC in an infundibulum in the upper pole of the right kidney (*arrow*)

diagnosis of collecting system filling defects is given in Table 11.1. Urothelial tumors are multifocal in 10–20% of cases and, therefore, should be high on the differential diagnosis of any process that produces multiple filling defects in the renal pelvis and ureter. Smaller filling defects may be better visualized with tomography (Fig. 11.11**).**

Stipple Sign

The stipple sign occurs when contrast is trapped within the interstices of a tumor and produces a stippled appearance [127, 128]. The stipple sign is highly suggestive of urothelial carcinoma but can also occur with other pathologies such as blood clots and fungus balls.

Ureteral Deviation

The course of the normal ureter is described in section The Normal Upper Urinary Tract. In most instances, the cause of ureteral deviation is ultimately determined by cross-sectional imaging. On IVP, both the direction of the ureteral deviation and the level at which it occurs are important and can suggest potential etiologies (Table 11.2).

Ureteral Dilation or Narrowing

Though the normal ureteral caliber has been defined by some uroradiologists as a ureter that is less than 8 mm in diameter,

Table 11.2 Differential diagnosis for ureteral deviation

Upper ureter
Medial
Renal parenchymal mass
Renal pelvic mass
Lateral retroperitoneal mass
Retroperitoneal fibrosis
Retrocaval ureter
Lateral
Congenital malformation of kidney
Horseshoe kidney
Malrotation
Renal pelvic mass
Retroperitoneal mass or lymph nodes
Psoas hypertrophy or abscess
Aortic aneurysm
Prior retroperitoneal surgery
Lower ureter
Medial
Pelvic lymphadenopathy
Pelvic mass
Prior pelvic surgery
Pelvic prolapse
Bladder diverticulum
Inguinal ureteral herniation
Lateral
Pelvic mass
Iliac artery aneurysm
Urinoma/Hematoma
Prior pelvic surgery
Femoral ureteral herniation

the best way to determine dilation is usually comparison to the contralateral side (Fig. 11.12) [108]. The ureter is often slightly dilated just above the area where it crosses the common iliac artery, a segment that has been called the ureteral spindle. Causes of ureteral dilation are given in Table 11.3. Narrowing of the ureter should be interpreted with caution because normal peristaltic waves may give the false impression of a narrowed segment (hence the importance of obtaining two views of any suspected pathology). Determining intrinsic from extrinsic causes of ureteral narrowing can be helpful. Intrinsic infiltration typically produces an irregular and abrupt change in ureteral caliber that resembles an apple core. Extrinsic encasement tends to produce a smooth tapering of the ureter. Causes of ureteral narrowing are given in Table 11.4.

Advantages of Ivp

Cost and Availability

Intravenous pyelography is inexpensive and can be obtained with a strict minimum of radiologic equipment. Even the most remote rural facilities can perform IVP if basic radiography is available.

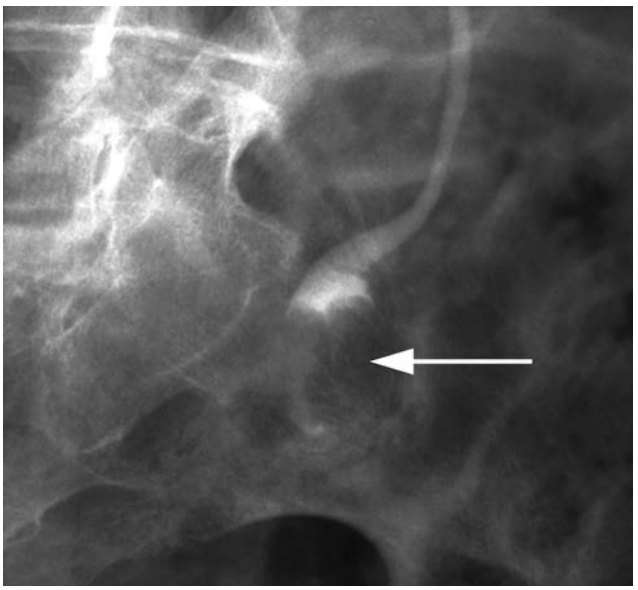

Fig. 11.12 Image from an intravenous pyelogram demonstrates a TCC filling the distal left ureter (*arrow*) with slight ureteral dilatation proximally

Table 11.3 Differential diagnosis for ureteral dilation

Obstructive
Intraluminal ureteral mass (see Table 11.1)
Extraluminal ureteral pathology
Ureteral stricture
Retroperitoneal or pelvic mass
Retroperitoneal fibrosis
Intravesical obstruction
Bladder tumor
Bladder calculus
Bladder infection (e.g., TB, schistosomiasis)
Neurogenic bladder (± detrusor-sphincter dysynergia)
Infravesical obstruction
Benign prostatic hyperplasia
Prostatic or urethral tumor
Urethral stricture
Non-obstructive
Pregnancy
Ureteral atony
Postobstructive residual dilation
Infection (endotoxin)
High urine flow
Polydipsia
Diabetes insipidus
Postobstructive diuresis
Congenital
Vesicoureteral reflux
Megaureter
Ectopic ureter
Ureterocele
Prune belly syndrome
Retrocaval ureter

Table 11.4 Differential diagnosis for ureteral narrowing

Normal
Ureteral peristalsis
Vascular imprinting
Neoplasia
Urothelial tumors
Retroperitoneal/pelvic tumor
Lymph nodes
Metastases
Stricture
Iatrogenic
Trauma
Radiation
Congenital
Infection
TB
Schistosomiasis
Inflammation
Malakoplakia
Endometriosis
Inflammatory bowel disease

Image Quality

Many physicians still regard IVP as one of the best tests for visualizing ureteral anatomy.

Disadvantages of IVP

Contrast Toxicity

A full discussion of the toxicities of radiocontrast is beyond the scope of this chapter and we provide only a brief overview here. The reader is referred to Bush and Lasser for a complete discussion [129]. Nephrotoxicity is probably the most important complication of IVP—though not the only one—and its incidence depends on the type and dose of contrast used, the underlying health of the patient at study, and the medication used by the patient. Numerous clinical

trials have been conducted in an attempt to find strategies to minimize this complication. European guidelines for the prevention of contrast nephrotoxicity have recently been published and propose the following important points [130]. Identifying individuals at risk of contrast nephrotoxicity prior to injecting contrast may reduce its incidence. Risk factors include diabetes, renal failure, congestive heart failure, dehydration, nephrotoxic drugs (e.g., NSAIDs, gentamicin), and age over 70. Physicians should try to minimize contrast nephrotoxicity by adopting a prevention strategy. Universal preventative measures include: ensuring adequate hydration (oral or IV), using low-osmolar contrast agents, minimizing contrast dose, maximizing time delay between contrast injections, stopping nephrotoxic drugs, avoiding diuretics, and avoiding contrast altogether if not necessary. Other interventions that have shown promise in randomized trials include intravenous bicarbonate infusions and *N*-acetylcysteine [131–134]. Another interesting investigational treatment with low toxicity is vitamin C [135].

Contrast Allergy

The incidence of anaphylactoid reactions to contrast media depends on the type of agent used and the patient's history of atopic reactions [136]. Most anaphylactoid reactions occur within minutes of contrast injection but some reactions may take up to 2 hours to develop [136]. Overall, the risk of any form of anaphylactoid reaction is 5% with ionic contrast and 1% with non-ionic contrast [136, 137]. Severe reactions are much less common, occurring in 1 in 750 patients injected with ionic contrast and in 1 in 3000 patients injected with non-ionic contrast [136, 137]. Risk factors for anaphylactoid reactions include asthma (RR=10), previous contrast reaction (RR=5), other allergies (RR=2.5), congestive heart disease, sickle cell anemia, anxiety, certain medications (β-blockers, IL-2, NSAIDs), and pheochromocytoma [136]. Patients with risk factors should receive a pre-contrast protocol of antihistamines and corticosteroids such as that supported by the European Society of Urogenital Radiology [138, 139].

Severe Obstruction

If the renal unit that is investigated is severely obstructed and no contrast is excreted into the collecting system by 10 minutes, delayed films will be required. Often these films do not adequately demonstrate the collecting system despite multiple radiation exposures, and alternative cross-sectional imaging studies become indicated. Unfortunately, the dose of contrast administered during IVP into the obstructed collecting system is quite high and may force delay of CT imaging by 1–2 days. This delay in diagnosis may prove quite distressing for both the physician and the patient.

Retrograde Pyelography

Brief History

Retrograde pyelography was described by the German physicians Fritz Voelcker and Alexander von Lichtenberg in 1906 and was the first technique used to specifically visualize the renal collecting system [98, 140]. The initial images of the ureter were the result of vesicoureteral reflux that occurred during a cystogram but this rapidly lead to the purposeful catheterization of the ureteral orifice and the retrograde injection of contrast media. The technique of retrograde pyelography was popularized in North America by William Braasch who practiced urology at the Mayo Clinic from 1907 to 1946 (Fig. 11.13). Braasch was a major advocate of retrograde pyelography and was responsible for describing the normal pyelographic upper tract anatomy and the use of pyelography for diagnosing malignant diseases of the genitourinary tract [141–143]. Improvements in contrast agents made over the next 100 years have made retrograde pyelography much safer for the patient.

Fig. 11.13 William Braasch, Mayo Clinic urologist, 1907–1946

Technique

Standard Single-Contrast Technique

Retrograde pyelography is a minimally invasive method of imaging the renal collecting system that generally requires cystoscopic visualization of the ureteral orifice, although there have been reports of performing the technique completely under fluoroscopic guidance [144, 145]. Regardless of the method employed, sterility is important because the introduction of bacteria directly into the renal collecting system and bloodstream is a potentially catastrophic complication. A small ureteral catheter, typically 4–7 F, is then slowly advanced into the distal intramural ureter. If urine collection, brush biopsy, or saline barbotage specimens are to be sent for cytologic analysis, as should routinely be the case if a tumor is on the differential diagnosis, these samples should be obtained prior to injecting contrast media into the collecting system. This is done because contrast media, particularly ionic agents with high osmolarity, can alter the cytologic appearance of normal urothelial cells resulting in a potential false-positive urine cytology [146–149]. Newer iso-osmolar contrast agents do not appear to have this problem [146]. Air bubbles in the ureteral catheter should be purged prior to inserting the catheter into the ureter because these can create the false impression of a filling defect, and positioning the patient in the Trendelenberg position may result in better opacification of the renal calyces. A scout film should be obtained prior to contrast injection to assess for mass effects and calcification. Under fluoroscopic guidance, 5–10 mL of diluted contrast media is then slowly injected at low pressure into the ureteral catheter. The ureter and renal pelvis are then assessed systematically. Rotating the fluoroscopy head can provide alternate views of the intrarenal collecting system and prove vital to correctly diagnosing pathology.

Double-Contrast Technique

The use of gas to visualize the urinary collecting system is called gas pyelography and the combination of a gas and a liquid contrast agent is referred to as double-contrast pyelography [150–154]. Several options exist for gas pyelography including oxygen, carbon dioxide, room air, and other inert gases. Carbon dioxide is preferred because it is safest. The technique for catheterizing the ureter is the same as described above with the exception of patient positioning: the reverse Trendelenberg position is preferred [154, 155]. A volume of 15–20 mL of gas is injected into the renal pelvis immediately following the injection of 5 mL of radiocontrast media. Though the risk of gas embolism with gas pyelography is not known with certainty, it has certainly been described and should be avoided at all costs [155–157]. The risk of gas embolism and little gain in diagnostic accuracy have made gas pyelography a largely unused procedure.

Imaging Features of Ureteral and Renal Pelvic Tumors

The imaging features of ureteral and renal pelvic tumors visualized with retrograde pyelography are generally the same as described earlier with intravenous urography. Tumors appear as filling defects, irregular stenoses, nonvisualized calyces, and hydronephrosis. The advantages of retrograde pyelography over other imaging modalities are discussed below. Two imaging features of ureteral tumors that are best detected with retrograde pyelography are the so-called goblet sign and Bergman's sign.

Goblet Sign

The goblet sign (a.k.a. chalice sign) refers to a cup-shaped collection of contrast media that is seen just distal to the intraluminal filling defect and suggests the presence of a tumor (Figs. 11.14 and 11.15) [158]. The slow growth of an intraluminal tumor causes proximal as well as distal expansion of the ureter [159]. Additionally, a pedunculated tumor may also be pushed distally during peristalsis only to return to its normal cephalad position between contractions [160]. Presence of the goblet sign suggests a superficial (i.e., less aggressive) tumor [158].

Bergman's Sign

Bergman's sign (a.k.a. catheter coiling sign) refers to the coiling of a ureteral catheter in the infratumoral ureter [159]. Its interpretation and cause are exactly the same as the goblet sign.

Advantages of Retrograde Pyelography

Fluoroscopic Monitoring

Fluoroscopic monitoring allows this imaging modality to better visualize the pathology in the urinary tract because the patient or fluoroscopy head can be repositioned to provide an optimal view of the problem. Often a slight change in the angle of view can result in a dramatically better picture of the pathologic process.

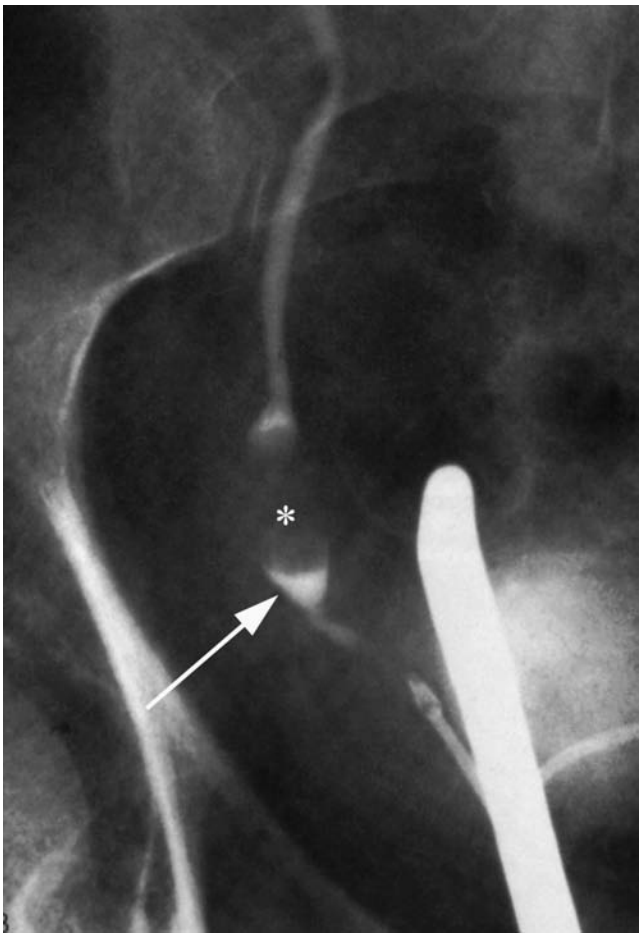

Fig. 11.14 Image from a retrograde pyelogram demonstrates a TCC filling the distal right ureter (*asterisk*) with slight ureteral dilatation distally (*arrow*). The distal ureteral dilation is known as the "chalice sign" or the "goblet sign"

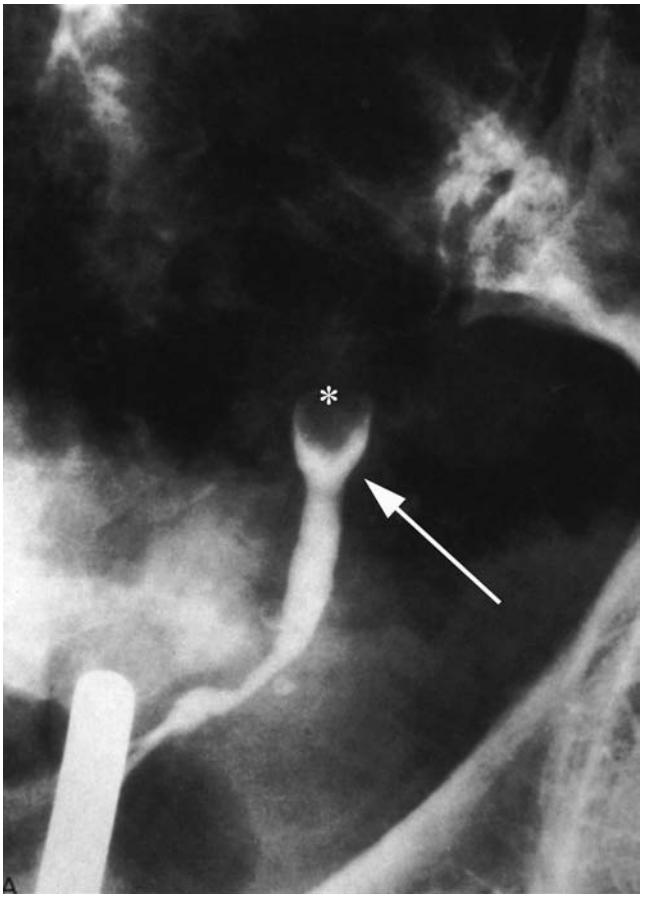

Fig. 11.15 Image from a retrograde pyelogram demonstrates a TCC filling the distal left ureter (*asterisk*) demonstrating the "goblet sign"

Intracavitary Filling

More contrast is instilled in the ureter and renal pelvis with retrograde pyelography than is possible with any intravascular imaging technique. This can sometimes be very useful in opacifying the phantom calyces seen on IVP. Many physicians feel that retrograde pyelography provides the best quality images of the renal pelvis and the most accurate measure of the extent of a ureteral tumor (i.e., length of ureteral involvement and multifocality) (Fig. 11.16).

Renal Failure

When renal function is so severely impaired that the kidney cannot excrete the contrast media or when intravascular contrast media risks worsening stable renal impairment, retrograde pyelography can be of use. As noted below, retrograde pyelography can worsen renal function, although this occurs very rarely. Most urologists and radiologists would agree that retrograde contrast injection is unlikely to cause significant renal dysfunction.

Contrast Toxicity

The injection of contrast media into the collecting system is associated with a very low adverse event rate. Despite this, there have been reports of a variety of contrast-related complications that deserve mention. Contrast nephrotoxicity can occur after retrograde pyelography and seems to be associated with bilateral obstruction, the presence of backflow (see later), and contrast-induced mucosal edema [161–163]. The course of resolution appears similar to that observed in cases of intravenous contrast nephrotoxicity.

Contrast Allergy

There is a very low rate of anaphylactoid reactions when contrast is administered directly into the urinary collecting system via retrograde injection. Though the urothelium

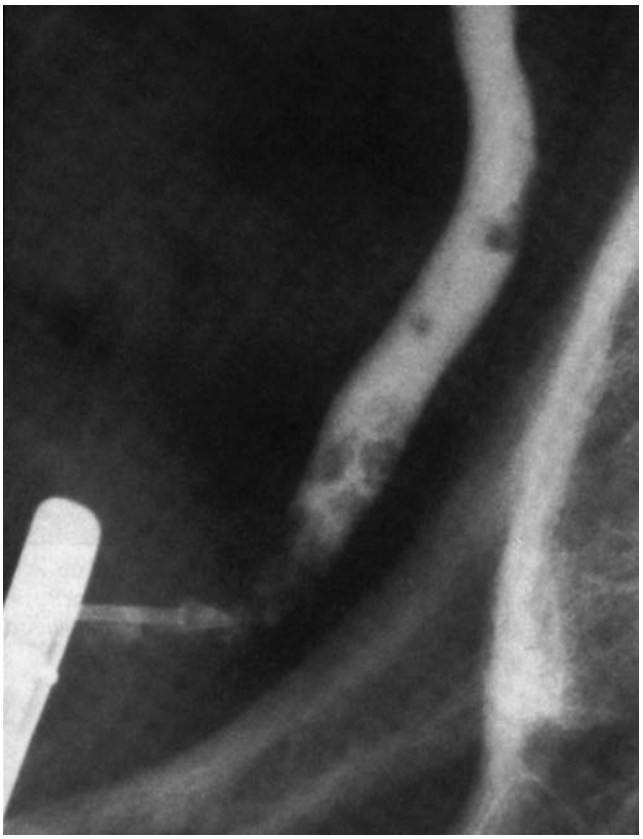

Fig. 11.16 Image from a retrograde pyelogram demonstrates multiple tiny papillary TCC in the distal left ureter

is considered a relatively impermeable barrier, contrast can be absorbed through the urothelium and enter the circulation [164–166]. Backflow mechanisms may also be involved in certain cases. A variety of allergic presentations have been described in patients undergoing cystography and retrograde pyelography, ranging from simple urticarial rashes to circulatory collapse [167–170]. Non-ionic contrast agents cause much fewer adverse reactions than ionic agents. It is unknown whether or not prophylaxis regimens are efficacious or indicated for preventing anaphylactoid reactions in patients undergoing cystography or retrograde pyelography [171]. Our bias is to err on the side of caution and administer prophylaxis to patients who have previously developed a reaction or that are at high risk of one.

Ancillary Diagnostic Procedures

Selective ureteral cytologies, saline barbotage, brush biopsy, and ureteroscopy can all be done in the same setting as retrograde pyelography. Combining all these diagnostic modalities provides a better chance of diagnosing difficult cases and is recommended in the follow-up of patients at high risk for an upper tract urothelial tumor [172].

Drainage

A ureteral stent can be placed into the ureter to relieve obstruction and symptoms caused by the tumor at the same time as retrograde pyelography.

Disadvantages of Retrograde Pyelography

Difficult Ureteral Orifice

All urologists with significant experience will recall occasions where ureteral cannulation was simply not possible. Some of the more common causes of difficult ureteral catheterization include a reimplanted ureter, the presence of a urinary diversion, a large prostate, a tumor at the ureteral orifice or previous transurethral resection thereof, a bladder diverticulum, extensive hematuria, an obstructing ureteral calculus, and looping dilated ureters. There are many tricks and tools that can assist in these situations but in certain cases the most rapid solution is to abort the procedure and obtain a percutaneous nephrostomy tract.

Iatrogenic Trauma

Though cystoscopy is a routine procedure for the urologist, inserting an instrument into the urethra should not be taken lightly. Many serious complications have occurred during cystoscopy and ureteral catheterization. Some of the more common complications include perforation of the urinary tract (urethra, bladder, ureter, or the renal pelvis) [173, 174], stricture with secondary obstruction [175–177], and infection/sepsis [178]. Although controversial, percutaneous nephrostomy is generally preferred over ureteral catheterization in the context of infected urine [179–182].

Backflow

Excessive injection pressure or trauma to the urothelium can result in the leakage of radiocontrast media into lymphovascular spaces [183–185]. This process is known as backflow and five distinct varieties have been described. *Pyelovenous backflow* occurs when contrast leaks into the venous drainage system of the kidney [186, 187]. It provides a direct route for contrast, air, and bacteria to enter the bloodstream. This is likely the point at which anaphylactoid reactions occur. Air embolism is a rare complication of retrograde pyelography that is related to pyelovenous backflow [157]. *Pyelolymphatic backflow* occurs when contrast leaks into the fine lymphatic channels that line the renal sinus and

migrates toward the hilar and retroperitoneal lymph nodes [186, 188]. Renal tubular toxicity has been reported to occur through this mechanism [163]. Backflow into a tumor has been termed *pyelocancerous backflow* [189, 190]. It is rare and of unknown significance. Intrarenal backflow refers to two things: pyelotubular backflow and pyelointerstitial backflow. *Pyelotubular backflow* occurs when contrast leaks into the collecting ducts and enters the nephron in a retrograde manner whereas *pyelointerstitial backflow* occurs when contrast leaks into the renal interstitium [184, 191]. Intrarenal backflow has been associated with impending renal transplant rejection [191, 192], renal ischemia [193–195], and prolonged obstruction [184]. The last form of backflow to be discussed is *pyelosinus backflow*. This form of backflow occurs when small tears in the calyces and renal pelvis develop and allow leakage of contrast into the renal sinus and the retroperitoneal space [196, 197]. The main clinical problems associated with this type of backflow are the development of a urinoma or retroperitoneal abscess [196, 198]. Though backflow can be prevented in most instances by keeping the intrapelvic pressure below 30 mmHg, some normal individuals will have backflow despite a perfect low-pressure technique.

Staging

Retrograde pyelography cannot establish extraureteral extension or the distant spread of a detected tumor. Occasionally retrograde pyelography will identify ureteral deviation caused by retroperitoneal lymph nodes or renal parenchymal invasion by a urothelial tumor, but these are the exceptions and always require cross-sectional imaging confirmation.

Carcinogenesis

A condition of historical interest is thorium-induced urothelial carcinoma. Thorotrast and Umbrathor were contrast agents composed of thorium dioxide, first introduced in 1915 and used routinely from the 1930s to the 1950s [199]. Thorium dioxide is mildly radioactive (it emits α-particles) and has a half-life of over 400 years. Small deposits of thorium (that are detectable by CT) occasionally formed under the urothelium of patients treated with this agent and many people developed cancers of the kidney and collecting system secondarily, 20–30 years after their exposure [200–204]. Newer contrast agents have not had this problem.

Antegrade Pyelography

Brief History

Percutaneous access to the upper urinary tract had its beginning in France in 1949 and was popularized by other groups in the mid-1950s [205–209]. The technique was initially used to diagnose and treat patients with severe hydronephrosis but has since been adapted to serve a wide variety of diagnostic and therapeutic needs [210]. Ultrasound or fluoroscopy guidance is now routinely used to help place the needle in the desired calyx [211–214].

Technique

Antegrade pyelography is generally reserved for patients that cannot receive intravenous contrast and that failed an attempt at retrograde pyelography. It can also be used as a primary imaging modality for patients with an obstruction of the upper urinary tract because the obstruction can be treated and its cause diagnosed.

Antegrade Pyelography

A quick focused medical history, a urine culture, and a coagulation profile are recommended prior to commencing this procedure. The patient is placed in the prone or prone-oblique position. Some form of imaging, usually ultrasonography or fluoroscopy, is used to guide the initial needle puncture into the desired renal calyx. When imaging or manometry are the only goals, a small 22- or 24-gauge needle may be sufficient to inject the contrast material and measure intrapelvic pressures. Strict sterility must be adhered to if infectious complications are to be avoided. To minimize the risk of bleeding complications, the needle tract is ideally placed through the relatively avascular line of Brödel on the posterolateral surface of the kidney [215, 216]. It is also generally preferred to target a posterior calyx in order to minimize the risk of bleeding and colonic injury [217, 218]. Similarly, infracostal puncture of a lower pole calyces is preferred over supracostal puncture of an upper pole calyx because of the risk of puncturing the pleura and the lung [219, 220]. Direct puncture of the renal pelvis should be avoided because of the risk of trauma to the central renal vasculature and the risks of urinoma and urinary fistula formation. Local anesthetics are usually adequate for pain control and their presence in the vicinity of the renal capsule is usually appreciated by the patient. Once the needle enters the collecting system, its position can be confirmed by the

respiratory motion of the needle and the appearance of the aspirated urine. Urine cultures and cytologies are almost always appropriate. Final confirmation of needle position is obtained by injecting a small dose of contrast into the collecting system and confirming its location with fluoroscopy.

Percutaneous Nephrostomy

When the renal unit in question is obstructed, it may be desirable to leave a nephrostomy tube to decompress the kidney and permit recovery of renal function. The nephrostomy tube can be used at a later date for performing antegrade pyelography or for endourologic access to the tumor. The technique for obtaining renal access is the same as that described above except that a slightly different needle is used. Once the needle is confirmed to be in the collecting system, a guidewire is inserted into the needle and positioned within the renal pelvis and ureter. The nephrostomy tract is then progressively dilated until an appropriately sized nephrostomy tube can be placed. Great care must be taken not to overdistend or puncture the renal pelvis during this procedure because serious bleeding and infection may result. The nephrostomy is then fixed to the skin in a manner that prevents inadvertent kinking, removal, or traction [221–223].

Imaging Features of Ureteral and Renal Pelvic Tumors

Urothelial tumors have essentially the same imaging characteristics with antegrade pyelography as with IVP and retrograde pyelography. As with retrograde pyelography, some physicians feel that direct injection of contrast into the collecting system provides for optimal anatomic detail (Fig. 11.17).

Advantages of Antegrade Pyelography

Success Rate

The success rate for establishing a percutaneous nephrostomy tract is over 99% and is relatively constant if the operator performs more than 10 nephrostomies per year [224–227]. The technique is therefore a very reliable way of diagnosing patients that have failed other imaging modalities.

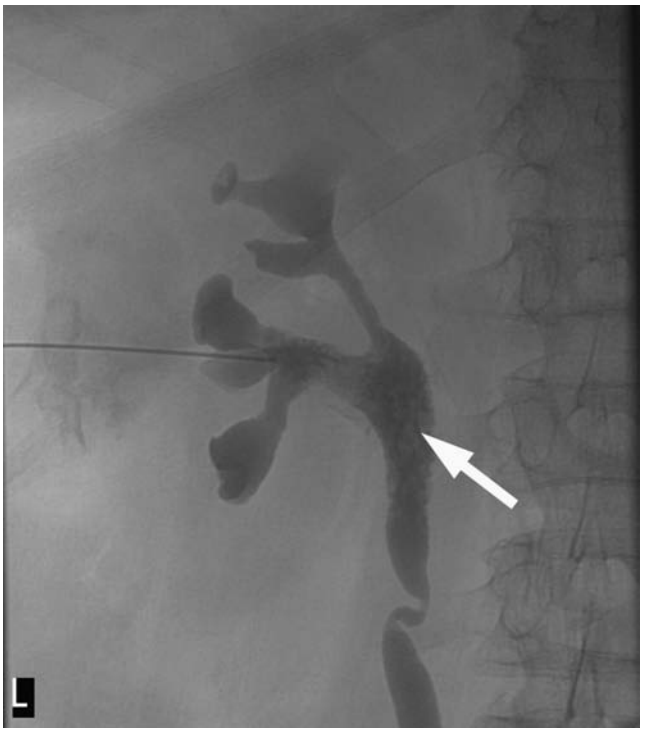

Fig. 11.17 Antegrade pyelogram demonstrating multiple tiny filling defects carpeting the right renal pelvis and upper right ureter (*arrow*) found to multifocal TCC at surgery

Drainage

The ability to leave a drainage nephrostomy catheter can be a major benefit, particularly for the patient with infected urine. There has been concern about the potential for tumor seeding along the nephrostomy tract [228–230]. This phenomenon appears to be quite rare and not all groups have observed it [231–235]. Nonetheless, for patients who eventually undergo nephroureterectomy, it may be wise to excise the nephrostomy tract. Brachytherapy has also been used to treat the nephrostomy tract in patients undergoing endourologic treatment [236].

Ancillary Diagnostic Procedures

As with retrograde pyelography, urine cultures, cytologies, and brush biopsies can all be obtained via the nephrostomy access [232]. A pressure-flow (Whittaker) study can also be performed if obstruction is questionable [237–242].

Treatment

The nephrostomy tract can be used for endourologic management of renal pelvic and upper ureteral tumors and chemotherapy and BCG can be dripped into the collecting

system safely via the nephrostomy [230, 231, 233, 235, 243–245].

Disadvantages of Antegrade Pyelography

Nearly all the disadvantages of this imaging approach are due to the potential complications associated with percutaneous renal access.

Bleeding

Hematuria is nearly universal after percutaneous needle puncture of the kidney but serious hemorrhage is fortunately uncommon. The incidence of major bleeding is directly related to the size of the nephrostomy tract. For small nephrostomy tracts (<12 F) the reported transfusion and/or intervention rates generally range from 1 to 4% while large tracts (>12 F) may have rates up to 20% [224, 225, 246–250]. The estimated average blood loss from a large nephrostomy tract ranges from 16 to 28 g/L [251, 252]. Risk factors for increased blood loss other than increasing nephrostomy tract size include renal pelvic perforation [251, 252], multiple renal punctures [251, 252], anterior calyx access [217], supracostal access [217, 220], diabetes [252], dilation of the nephrostomy tract without a balloon [248], and the lack of imaging guidance [213, 252]. Most renal hemorrhages can be handled non-operatively and we suggest a stepwise approach to management. Simple maneuvers such as clamping the nephrostomy tube and balloon tamponade should be considered first [249, 253, 254]. For procedures conducted in the operative setting, simple cauterization of the bleeding vessel or the application of fibrin glue may be of value [255–258]. If these methods fail or if the bleeding is too brisk to warrant an initial conservative approach, vascular access and selective renal embolization should be attempted [247, 249, 259–264]. Renal embolization is generally well tolerated but renal infarction of varying degrees of severity can occur [265, 266]. Other complications that have been reported secondary to endovascular techniques include pseudoaneurysm or arteriovenous fistula formation at the access site [267–270], thrombosis and dissection of the aorta [271, 272], and embolization of the limbs [273]. Lastly, severe bleeding can be associated with the formation of a retroperitoneal hematoma [274, 275]. These hematomas can be a source of pain and a nidus for infection.

Arteriovenous Fistula

AV fistulae are usually clinical entities that escape clinical attention. The incidence of radiologic AV fistula occurring after nephrostomy is unknown but reaches 10–15% for renal biopsies [276–279]. Most of these cases resolve spontaneously within 6–12 months but may occasionally require embolization or surgical treatment [280, 281].

Iatrogenic Organ Injury

Any organ that lies in or near the retroperitoneum can be punctured while obtaining percutaneous access to the kidney. The most commonly injured organs are the renal pelvis [224], the colon [218, 282–285], the liver [286, 287], the spleen [286–289], and pleura/lung [219, 220, 250, 287, 290–293].

Death

The death rate from percutaneous nephrostomies is very low but is not zero. Large series report death rates in the 0.1–0.5% range [224, 250].

Conclusions

The traditional diagnostic modalities of IVP and retrograde pyelography are rapidly being replaced as first-line diagnostic modalities for flank pain and hematuria by CT and MR urography. In many circumstances, however, they may still be the optimal method of evaluating the upper urinary tract for the presence of a urothelial tumor. Table 11.5 shows the relative strengths and weaknesses of the various imaging techniques that can be used to identify upper urinary tract tumors.

Table 11.5 Strengths of various imaging modalities for upper urinary tract tumors

	IVP	Retrograde/antegrade	US	CT	MRI
Renal pelvis	+++	+++	+	++	++
Ureter	+++	+++	+	++	++
Calculi	++	++	+	+++	+
Staging	+	+	++	+++	+++
Cost	+++	+	+++	++	+
Radiation	++	++	+++	+	+++

References

1. Emamian SA, Nielsen MB, Pedersen JF, Ytte L. Kidney dimensions at sonography: correlation with age, sex, and habitus in 665 adult volunteers. AJR Am J Roentgenol. 1993;160(1):83–6.
2. Sanders RC, Conrad MR. The ultrasonic characteristics of the renal pelvicalyceal echo complex. J Clin Ultrasound. 1977;5(6):372–7.
3. Erwin BC, Carroll BA, Sommer FG. Renal colic: the role of ultrasound in initial evaluation. Radiology. 1984;152(1):147–50.
4. Szabo V, Sobel M, Legradi J, Balogh F. Diagnostic ultrasound in urology. Int Urol Nephrol. 1980;12(4):291–309.
5. Ellenbogen PH, Scheible FW, Talner LB, Leopold GR: sensitivity of gray scale ultrasound in detecting urinary tract obstruction. AJR Am J Roentgenol. 1978;130(4):731–3.
6. Amis ES Jr, Cronan JJ, Pfister RC, Yoder IC. Ultrasonic inaccuracies in diagnosing renal obstruction. Urology. 1982;19(1):101–5.
7. Harzmann R, Weckermann D. Importance of Doppler sonography in urology. Urol Int. 1990;45(4):258–63.
8. Tublin ME, Bude RO, Platt JF. Review: the resistive index in renal Doppler sonography: where do we stand? AJR Am J Roentgenol. 2003;180(4):885–92.
9. Kalmon EH, Albers DD, Dunn JH. Ureteral jet phenomenon: stream of opaque medium simulating an anomalous configuration of the ureter. Radiology. 1955;65:933–5.
10. Chiu NT, Wu CC, Yao WJ, et al. Evaluation and validation of ureteric jet index by glomerular filtration rate. Invest Radiol. 1999;34(8):499–02.
11. Rha SE, Byun JY, Jung SE, et al. The renal sinus: pathologic spectrum and multimodality imaging approach. Radiographics. 2004;24 Suppl 1:S117–31.
12. Arger PH, Mulhern CB, Pollack HM, Banner MP, Wein AJ. Ultrasonic assessment of renal transitional cell carcinoma: preliminary report. AJR Am J Roentgenol. 1979;132(3):407–11.
13. Subramanyam BR, Raghavendra BN, Madamba MR. Renal transitional cell carcinoma: sonographic and pathologic correlation. J Clin Ultrasound. 1982;10(5):203–10.
14. Wicks JD, Silver TM, Bree RL. Gray scale features of hematomas: an ultrasonic spectrum. AJR Am J Roentgenol. 1978;131(6):977–80.
15. Rosenfield AT, Taylor KJ, Dembner AG, Jacobson P. Ultrasound of renal sinus: new observations. AJR Am J Roentgenol. 1979;133(3):441–8.
16. Pollack HM, Arger PH, Goldberg BB, Mulholland SG. Ultrasonic detection of nonopaque renal calculi. Radiology. 1978;127(1):233–7.
17. Edell S, Zegel H. Ultrasonic evaluation of renal calculi. AJR Am J Roentgenol. 1978;130(2):261–3.
18. Mulholland SG, Arger PH, Goldberg BB, Pollack HM. Ultrasonic differentiation of renal pelvic filling defects. J Urol. 1979;122(1):14–6.
19. Gibson MS, Puckett ML, Shelly ME. Renal tuberculosis. Radiographics. 2004;24(1):251–6.
20. Kim SH, Yoon HK, Park JH, et al. Tuberculous stricture of the urinary tract: antegrade balloon dilation and ureteral stenting. Abdom Imaging. 1993;18(2):186–90.
21. Kollins SA, Hartman GW, Carr DT, Segura JW, Hattery RR. Roentgenographic findings in urinary tract tuberculosis. A 10 year review. Am J Roentgenol Radium Ther Nucl Med. 1974;121(3):487–99.
22. Dittrich M, Doehring E. Ultrasonographical aspects of urinary schistosomiasis: assessment of morphological lesions in the upper and lower urinary tract. Pediatr Radiol. 1986;16(3):225–30.
23. Ghoneim MA, Ashamallah A, Khalik MA. Bilharzial strictures of the ureter presenting with anuria. Br J Urol. 1971;43(4):439–43.
24. Gupta R, Kehinde EO, Sinan T, Al-Essa AA. Urinary schistosomiasis: urographic features and significance of drooping kidney appearance. Int Urol Nephrol. 2001;33(3):461–5.
25. Jorulf H, Lindstedt E. Urogenital schistosomiasis: CT evaluation. Radiology. 1985;157(3):745–9.
26. Dinsmore BJ, Pollack HM, Banner MP. Calcified transitional cell carcinoma of the renal pelvis. Radiology. 1988;167(2):401–4.
27. Li MK, Cheung WL. Squamous cell carcinoma of the renal pelvis. J Urol. 1987;138(2):269–71.
28. Blacher EJ, Johnson DE, Abdul-Karim FW, Ayala AG. Squamous cell carcinoma of renal pelvis. Urology. 1985;25(2):124–6.
29. Dumbadze I, Crawford ED, Mulvaney WP. Giant dendritic struvite calculus associated with transitional cell carcinoma of the ipsilateral renal pelvis and bladder: a case report and review of the literature. J Urol. 1979;122(5):692–3.
30. Lee TY, Ko SF, Wan YL, et al. Renal squamous cell carcinoma: CT findings and clinical significance. Abdom Imaging. 1998;23(2):203–8.
31. Katz R, Gofrit ON, Golijanin D, et al. Urothelial cancer of the renal pelvis in percutaneous nephrolithotomy patients. Urol Int. 2005;75(1):17–20.
32. Janetschek G, Putz A, Feichtinger H. Renal transitional cell carcinoma mimicking stone echoes. J Ultrasound Med. 1988;7(2):83–6.
33. Seong CK, Kim SH, Lee JS, Kim KH, Sim JS, Chang KH. Hypoechoic normal renal sinus and renal pelvis tumors: sonographic differentiation. J Ultrasound Med. 2002;21(9):993–9; quiz 1001–2.
34. Kier R, Taylor KJ, Feyock AL, Ramos IM. Renal masses: characterization with Doppler US. Radiology. 1990;176(3):703–7.
35. Kuijpers D, Jaspers R. Renal masses: differential diagnosis with pulsed doppler US. Radiology. 1989;170(1 Pt 1):59–60.
36. Horstman WG, McFarland RM, Gorman JD. Color Doppler sonographic findings in patients with transitional cell carcinoma of the bladder and renal pelvis. J Ultrasound Med. 1995;14(2):129–33.
37. Kim HJ, Lim JW, Lee DH, Ko YT, Oh JH, Kim YW. Transitional cell carcinoma involving the distal ureter: assessment with transrectal and color doppler ultrasonography. J Ultrasound Med. 2005;24(12):1625–33.
38. Killi RM, Cal C, Pourbagher A, Yurtseven O. Doppler sonographic diagnosis of primary transitional cell carcinoma of the ureter. J Clin Ultrasound. 2000;28(7):361–4.
39. Bree RL, Schultz SR, Hayes R. Large infiltrating renal transitional cell carcinomas: CT and ultrasound features. J Comput Assist Tomogr. 1990;14(3):381–5.
40. Igarashi T, Muakami S, Shichijo Y, Matsuzaki O, Isaka S, Shimazaki J. Clinical and radiological aspects of infiltrating transitional cell carcinoma of the kidney. Urol Int. 1994;52(4):181–4.
41. Fukuya T, Honda H, Nakata H, et al. Computed tomographic findings of invasive transitional cell carcinoma in the kidney. Radiat Med. 1994;12(1):6–10.
42. Hadas-Halpern I, Farkas A, Patlas M, Zaghal I, Sabag-Gottschalk S, Fisher D. Sonographic diagnosis of ureteral tumors. J Ultrasound Med. 1999;18(9):639–45.
43. Voet D, Mareels S, Oosterlinck W, Afschrift M. Sonographic diagnosis of a nonobstructive tumor in the mid-ureter. J Clin Ultrasound. 1997;25(8):459–60.
44. Barnett SB. Biophysical aspects of diagnostic ultrasound. Ultrasound Med Biol. 2000;26 Suppl 1:S68–70.
45. Dendy PP, Brugmans MJ. Low dose radiation risks. Br J Radiol. 2003;76(910):674–7.
46. Berrington de Gonzalez A, Darby S. Risk of cancer from diagnostic X-rays: estimates for the UK and 14 other countries. Lancet. 2004;363(9406):345–51.
47. Wakeford R. The cancer epidemiology of radiation. Oncogene. 2004;23(38):6404–28.

48. Brenner DJ, Doll R, Goodhead DT, et al. Cancer risks attributable to low doses of ionizing radiation: assessing what we really know. Proc Natl Acad Sci USA. 2003;100(24):13761–6.
49. Sheafor DH, Hertzberg BS, Freed KS, et al. Nonenhanced helical CT and US in the emergency evaluation of patients with renal colic: prospective comparison. Radiology. 2000;217(3):792–7.
50. Ripolles T, Agramunt M, Errando J, Martinez MJ, Coronel B, Morales M. Suspected ureteral colic: plain film and sonography vs unenhanced helical CT. a prospective study in 66 patients. Eur Radiol. 2004;14(1):129–36.
51. Fowler KA, Locken JA, Duchesne JH, Williamson MR. US for detecting renal calculi with nonenhanced CT as a reference standard. Radiology. 2002;222(1):109–13.
52. Remer EM, Herts BR, Streem SB, et al. Spiral noncontrast CT versus combined plain radiography and renal US after extracorporeal shock wave lithotripsy: cost-identification analysis. Radiology. 1997;204(1):33–7.
53. Hamm M, Wawroschek F, Weckermann D, et al. Unenhanced helical computed tomography in the evaluation of acute flank pain. Eur Urol. 2001;39(4):460–5.
54. Heidenreich A, Desgrandschamps F, Terrier F. Modern approach of diagnosis and management of acute flank pain: review of all imaging modalities. Eur Urol. 2002;41(4):351–62.
55. Grossfeld GD, Litwin MS, Wolf JS Jr, et al. Evaluation of asymptomatic microscopic hematuria in adults: the American Urological Association best practice policy—part II: patient evaluation, cytology, voided markers, imaging, cystoscopy, nephrology evaluation, and follow-up. Urology. 2001;57(4):604–10.
56. Delorme S, van Kaick G. Imaging of abdominal nodal spread in malignant disease. Eur Radiol. 1996;6(3):262–74.
57. Williams AD, Cousins C, Soutter WP, et al. Detection of pelvic lymph node metastases in gynecologic malignancy: a comparison of CT, MR imaging, and positron emission tomography. AJR Am J Roentgenol. 2001;177(2):343–8.
58. Grubnic S, Vinnicombe SJ, Norman AR, Husband JE. MR evaluation of normal retroperitoneal and pelvic lymph nodes. Clin Radiol. 2002;57(3):193–200; discussion 201–4.
59. Bellin MF, Lebleu L, Meric JB. Evaluation of retroperitoneal and pelvic lymph node metastases with MRI and MR lymphangiography. Abdom Imaging. 2003;28(2):155–63.
60. Friedland GW. Staging of genitourinary cancers. The role of diagnostic imaging. Cancer. 1987;60(3 Suppl):450–8.
61. Wernecke K, Rummeny E, Bongartz G, et al. Detection of hepatic masses in patients with carcinoma: comparative sensitivities of sonography, CT, and MR imaging. AJR Am J Roentgenol. 1991;157(4):731–9.
62. Heiken JP, Weyman PJ, Lee JK, et al. Detection of focal hepatic masses: prospective evaluation with CT, delayed CT, CT during arterial portography, and MR imaging. Radiology. 1989;171(1):47–51.
63. Hohmann J, Albrecht T, Hoffmann CW, Wolf KJ. Ultrasonographic detection of focal liver lesions: increased sensitivity and specificity with microbubble contrast agents. Eur J Radiol. 2003;46(2):147–59.
64. Davis SD. CT evaluation for pulmonary metastases in patients with extrathoracic malignancy. Radiology. 1991;180(1):1–12.
65. Chalmers N, Best JJ. The significance of pulmonary nodules detected by CT but not by chest radiography in tumour staging. Clin Radiol. 1991;44(6):410–2.
66. Herold CJ, Bankier AA, Fleischmann D. Lung metastases. Eur Radiol. 1996;6(5):596–606.
67. Miyazato M, Yonou H, Sugaya K, Koyama Y, Hatano T, Ogawa Y. Transitional cell carcinoma of the renal pelvis forming tumor thrombus in the vena cava. Int J Urol. 2001;8(10):575–7.
68. Spahn M, Portillo FJ, Michel MS, et al. Color Duplex sonography vs. computed tomography: accuracy in the preoperative evaluation of renal cell carcinoma. Eur Urol. 2001;40(3):337–42.
69. Solwa Y, Sanyika C, Hadley GP, Corr P. Colour Doppler ultrasound assessment of the inferior vena cava in patients with Wilms' tumour. Clin Radiol. 1999;54(12):811–4.
70. Bos SD, Mensink HJ. Can duplex Doppler ultrasound replace computerized tomography in staging patients with renal cell carcinoma? Scand J Urol Nephrol. 1998;32(2):87–91.
71. Habboub HK, Abu-Yousef MM, Williams RD, See WA, Schweiger GD. Accuracy of color Doppler sonography in assessing venous thrombus extension in renal cell carcinoma. AJR Am J Roentgenol. 1997;168(1):267–71.
72. Smith-Bindman R, Hosmer WD, Caponigro M, Cunningham G. The variability in the interpretation of prenatal diagnostic ultrasound. Ultrasound Obstet Gynecol. 2001;17(4):326–32.
73. Mikkonen RH, Kreula JM, Virkkunen PJ. Reproducibility of Doppler ultrasound measurements. Acta Radiol. 1996;37(4): 545–50.
74. Mikkonen RH, Kreula JM, Virkkunen PJ. Reliability of Doppler ultrasound in follow-up studies. Acta Radiol. 1998;39(2):193–9.
75. Ablett MJ, Coulthard A, Lee RE, et al. How reliable are ultrasound measurements of renal length in adults? Br J Radiol. 1995;68(814):1087–9.
76. Emamian SA, Nielsen MB, Pedersen JF. Intraobserver and interobserver variations in sonographic measurements of kidney size in adult volunteers. a comparison of linear measurements and volumetric estimates. Acta Radiol. 1995;36(4):399–401.
77. Goldberg BB, Bagley D, Liu JB, Merton DA, Alexander A, Kurtz AB. Endoluminal sonography of the urinary tract: preliminary observations. AJR Am J Roentgenol. 1991;156(1):99–103.
78. Goldberg BB, Liu JB, Merton DA, Kurtz AB. Endoluminal US: experiments with nonvascular uses in animals. Radiology. 1990;175(1):39–43.
79. Zeltser IS, Liu JB, Bagley DH. The incidence of crossing vessels in patients with normal ureteropelvic junction examined with endoluminal ultrasound. J Urol. 2004;172(6 Pt 1):2304–7.
80. Bagley DH, Liu JB, Grasso M, Goldberg BB. Endoluminal sonography in evaluation of the obstructed ureteropelvic junction. J Endourol. 1994;8(4):287–92.
81. Bagley DH, Liu JB, Goldberg B. Endoluminal sonographic imaging of the ureteropelvic junction. J Endourol. 1996;10(2):105–10.
82. Siegel CL, McDougall EM, Middleton WD, et al. Preoperative assessment of ureteropelvic junction obstruction with endoluminal sonography and helical CT. AJR Am J Roentgenol. 1997;168(3):623–6.
83. Keeley FX Jr, Moussa SA, Miller J, Tolley DA. A prospective study of endoluminal ultrasound versus computerized tomography angiography for detecting crossing vessels at the ureteropelvic junction. J Urol. 1999;162(6):1938–41.
84. Holm HH, Torp-Pedersen S, Larsen T, Dorph S. Transabdominal and endoluminal ultrasonic scanning of the lower ureter. Scand J Urol Nephrol Suppl. 1994;157:19–25.
85. Liu JB, Bagley DH, Conlin MJ, Merton DA, Alexander AA, Goldberg BB. Endoluminal sonographic evaluation of ureteral and renal pelvic neoplasms. J Ultrasound Med. 1997;16(8):515–21; quiz 523–4.
86. Grotas A, Grasso M. Endoluminal sonographic imaging of upper urinary tract: three-dimensional reconstruction. J Endourol. 2001;15(5):485–8.
87. Bagley DH, Liu JB. Three-dimensional endoluminal ultrasonography of the ureter. J Endourol. 1998;12(5):411–6.
88. Blomley MJ, Cooke JC, Unger EC, Monaghan MJ, Cosgrove DO. Microbubble contrast agents: a new era in ultrasound. BMJ. 2001;322(7296):1222–5.

89. Jakobsen JA, Correas JM. Ultrasound contrast agents and their use in urogenital radiology: status and prospects. Eur Radiol. 2001;11(10):2082–91.
90. Calliada F, Campani R, Bottinelli O, Bozzini A, Sommaruga MG. Ultrasound contrast agents: basic principles. Eur J Radiol. 1998;27 Suppl 2:S157–60.
91. Cosgrove D, Blomley M. Liver tumors: evaluation with contrast-enhanced ultrasound. Abdom Imaging. 2004;29(4):446–54.
92. Nicolau C, Bru C. Focal liver lesions: evaluation with contrast-enhanced ultrasonography. Abdom Imaging. 2004;29(3):348–59.
93. Chomas JE, Pollard RE, Sadlowski AR, Griffey SM, Wisner ER, Ferrara KW. Contrast-enhanced US of microcirculation of superficially implanted tumors in rats. Radiology. 2003;229(2): 439–46.
94. Kmetec A, Bren AF, Kandus A, Fettich J, Buturovic-Ponikvar J. Contrast-enhanced ultrasound voiding cystography as a screening examination for vesicoureteral reflux in the follow-up of renal transplant recipients: a new approach. Nephrol Dial Transplant. 2001;16(1):120–3.
95. Ascenti G, Zimbaro G, Mazziotti S, Chimenz R, Baldari S, Fede C. Vesicoureteral reflux: comparison between urosonography and radionuclide cystography. Pediatr Nephrol. 2003;18(8):768–71.
96. Valentini AL, De Gaetano AM, Minordi LM, et al. Contrast-enhanced voiding US for grading of reflux in adult patients prior to antireflux ureteral implantation. Radiology. 2004;233(1):35–9.
97. Liang HD, Blomley MJ. The role of ultrasound in molecular imaging. Br J Radiol. 2003;76 Spec No 2:S140–50.
98. Voelcker F, von Lichtenberg A. Pyelographie röntgenographie des neirenbeckens nach Kollargolfullung. Munch Med Wochenschr. 1906;53:105–6.
99. Cameron DF. Aqueous solutions of potassium and sodium iodides as opaque mediums in roentgenography. JAMA. 1918;70(11):754–5.
100. Osborne ED, Sutherland CG, Scholl AJ, Rowntree LG. Roentgenography of urinary tract during excretion of sodium iodide. JAMA. 1923;80(6):368–73.
101. Swick M. Intravenous urography by means of the sodium salt 5-iodo-2-pyridon-N-acetic acid. JAMA. 1930;95:1403–9.
102. Amis ES Jr. Epitaph for the urogram. Radiology. 1999;213(3):639–40.
103. Pollack HM, Banner MP. Current status of excretory urography. a premature epitaph? Urol Clin North Am. 1985;12(4):585–601.
104. Kumar R, Schreiber MH. The changing indications for excretory urography. JAMA. 1985;254(3):403–5.
105. Dalla Palma L. What is left of i.v. urography? Eur Radiol. 2001;11(6):931–9.
106. Choyke PL. The urogram: are rumors of its death premature? Radiology. 1992;184(1):33–4.
107. Hattery RR, King BF. Invited commentary. Radiographics. 2001;21(4):822–3.
108. Dyer RB, Chen MY, Zagoria RJ. Intravenous urography: technique and interpretation. Radiographics. 2001;21(4):799–21; discussion 822–4.
109. Hattery RR, Williamson B Jr, Hartman GW, LeRoy AJ, Witten DM. Intravenous urographic technique. Radiology. 1988;167(3):593–9.
110. Moody TE, Vaughn ED Jr, Gillenwater JY. Relationship between renal blood flow and ureteral pressure during 18 hours of total unilateral uretheral occlusion. Implications for changing sites of increased renal resistance. Invest Urol. 1975;13(3):246–51.
111. Vaughan ED Jr, Shenasky JH II, Gillenwater JY. Mechanism of acute hemodynamic response to ureteral occlusion. Invest Urol. 1971;9(2):109–18.
112. Vaughan ED Jr, Sorenson EJ, Gillenwater JY. Effects of acute and chronic ureteral obstruction on renal hemodynamics and function. Surg Forum. 1968;19:536–8.
113. Moody TE, Vaughan ED Jr, Gillenwater JY. Comparison of the renal hemodynamic response to unilateral and bilateral ureteral occlusion. Invest Urol. 1977;14(6):455–9.
114. Vaughan ED Jr, Sorenson EJ, Gillenwater JY. The renal hemodynamic response to chronic unilateral complete ureteral occlusion. Invest Urol. 1970;8(1):78–90.
115. Erden A, Fitoz S, Karagulle T, Tukel S, Akyar S. Radiological findings in the diagnosis of genitourinary candidiasis. Pediatr Radiol. 2000;30(12):875–7.
116. Adams FG, Murray RM. The radiological diagnosis of analgesic nephropathy. Clin Radiol. 1975;26(3):417–27.
117. Hare WS, Poynter JD. The radiology of renal papillary necrosis as seen in analgesic nephropathy. Clin Radiol. 1974;25(4):423–43.
118. Lindvall N. Radiological changes of renal papillary necrosis. Kidney Int. 1978;13(1):93–106.
119. Vijayaraghavan SB, Kandasamy SV, Mylsamy A, Prabhakar M. Sonographic features of necrosed renal papillae causing hydronephrosis. J Ultrasound Med. 2003;22(9):951–6; quiz 957–8.
120. Siegel MJ, McAlister WH. Calyceal diverticula in children: unusual features and complications. Radiology. 1979;131(1): 79–82.
121. Devine CJ Jr, Guzman JA, Devine PC, Poutasse EF. Calyceal diverticulum. J Urol. 1969;101(1):8–11.
122. Brennan RE, Pollack HM. Nonvisualized (“phantom”) renal calyx: causes and radiological approach to diagnosis. Urol Radiol. 1979;1(1):17–23.
123. Fein AB, McClennan BL. Solitary filling defects of the ureter. Semin Roentgenol. 1986;21(3):201–13.
124. Pollack HM, Arger PH, Banner MP, Mulhern CB Jr, Coleman BG. Computed tomography of renal pelvic filling defects. Radiology. 1981;138(3):645–51.
125. Parienty RA, Ducellier R, Pradel J, Lubrano JM, Coquille F, Richard F. Diagnostic value of CT numbers in pelvocalyceal filling defects. Radiology. 1982;145(3):743–7.
126. Lowe PP, Roylance J. Transitional cell carcinoma of the kidney. Clin Radiol. 1976;27(4):503–12.
127. McLean GK, Pollack HM, Banner MP. The “stipple sign”; - urographic harbinger of transitional cell neoplasms. Urol Radiol. 1979;1(2):77–9.
128. Gee J, Larsen CR, Silverman ML, Bihrle W III. Urothelial striations in a patient with transitional cell carcinoma in situ involving the ureter. J Urol. 1999;161(4):1279–80.
129. Bush WH, Lasser EC. Adverse reactions to intravascular iodinated contrast material. In: Pollack HM, McClennan BL, editors. Clinical urography. 2nd ed. Philadelphia: W.B. Saunders Company; 2000. pp. 43–66.
130. Thomsen HS, Morcos SK. Contrast media and the kidney: European Society of Urogenital Radiology (ESUR) guidelines. Br J Radiol. 2003;76(908):513–8.
131. Merten GJ, Burgess WP, Gray LV, et al. Prevention of contrast-induced nephropathy with sodium bicarbonate: a randomized controlled trial. JAMA. 2004;291(19):2328–34.
132. Tepel M, van der Giet M, Schwarzfeld C, Laufer U, Liermann D, Zidek W. Prevention of radiographic-contrast-agent-induced reductions in renal function by acetylcysteine. N Engl J Med. 2000;343(3):180–4.
133. Kay J, Chow WH, Chan TM, et al. Acetylcysteine for prevention of acute deterioration of renal function following elective coronary angiography and intervention: a randomized controlled trial. JAMA. 2003;289(5):553–8.
134. Pannu N, Manns B, Lee H, Tonelli M. Systematic review of the impact of N-acetylcysteine on contrast nephropathy. Kidney Int. 2004;65(4):1366–74.
135. Spargias K, Alexopoulos E, Kyrzopoulos S, et al. Ascorbic acid prevents contrast-mediated nephropathy in patients with renal

dysfunction undergoing coronary angiography or intervention. Circulation. 2004;110(18):2837–42.
136. Hagan JB. Anaphylactoid and adverse reactions to radiocontrast agents. Immunol Allergy Clin North Am. 2004;24(3):507–19, vii–viii.
137. Cochran ST. Anaphylactoid reactions to radiocontrast media. Curr Allergy Asthma Rep. 2005;5(1):28–31.
138. Thomsen HS, Morcos SK. Prevention of generalized reactions to CM. Acad Radiol. 2002;9 Suppl 2:S433–5.
139. Morcos SK, Thomsen HS, Webb JA. Prevention of generalized reactions to contrast media: a consensus report and guidelines. Eur Radiol. 2001;11(9):1720–8.
140. Skrepetis K, Siafakas I, Lykourinas M. Evolution of retrograde pyelography and excretory urography in the early 20th century. J Endourol. 2001;15(7):691–6.
141. Braasch WF, Carman RD. The pyelographic and roentgenologic diagnosis of renal tumors. Radiology. 1925;4(6):445–52.
142. Braasch WF. Pyelography (pyelo-ureterography) a study of the normal and pathologic anatomy of the renal pelvis and ureter. 1st ed. Philadelphia: Saunders; 1915.
143. Braasch WF, Hager BH. Urography. 2nd ed. Philadelphia: Saunders; 1927.
144. Babel SG, Winterkorn KG. Retrograde catheterization of the ureter without cystoscopic assistance: preliminary experience. Radiology. 1993;187(2):547–9.
145. Banner MP, Amendola MA, Pollack HM. Anastomosed ureters: fluoroscopically guided transconduit retrograde catheterization. Radiology. 1989;170(1 Pt 1):45–9.
146. Andriole GL, McClennan BL, Becich MJ, Picus DD. Effect of low osmolar, ionic and nonionic, contrast media on the cytologic features of exfoliated urothelial cells. Urol Radiol. 1989;11(3):133–5.
147. Fischer S, Nielsen ML, Clausen S, Vogelsang M, Hogsborg E. Increased abnormal urothelial cells in voided urine following excretory urography. Acta Cytol. 1982;26(2):153–8.
148. Barry JM, Murphy JB, Nassir E, Dawson P, Hodges CV. The influence of retrograde contrast medium on urinary cytodiagnosis: a preliminary report. J Urol. 1978;119(5):633–4.
149. McClennan BL, Oertel YC, Malmgren RA, Mendoza M. The effect of water soluble contrast material on urine cytology. Acta Cytologica. 1978;22(4):230–3.
150. Ricketts HJ, Rudd TG, Marcus VL, Krieger JN. Pneumopyelography: an adjunct to percutaneous nephrostomy and nephrolithotomy. AJR Am J Roentgenol. 1984;143(5):1093–5.
151. Izquierdo F, Rousaud A, Garat JM. Intraoperative pneumopyelography. Eur Urol. 1982;8(3):148–9.
152. Khan AU, Leary FJ, Greene LF. Pneumopyelography. Urology. 1976;8(1):92–3.
153. Fischel RE, Pikielny SS. Giant congenital calyceal diverticulum visualised by retrograde pneumopyelography. Br J Radiol. 1962;35:647–9.
154. Christiansen J. Retrograde pyelography with double contrast. A preliminary report. Acta Chir Scand. 1970;136(5):435–9.
155. Christiansen J. Retrograde pyelography with gas (carbon dioxide) as contrast medium. Acta Chir Scand. 1970;136(5):441–5.
156. Varkarakis J, Su LM, Hsu TH. Air embolism from pneumopyelography. J Urol. 2003;169(1):267.
157. Pyron CL, Segal AJ. Air embolism: a potential complication of retrograde pyelography. J Urol. 1983;130(1):125–6.
158. Daniels RE III. The goblet sign. Radiology. 1999;210(3):737–8.
159. Bergman H, Friedenberg RM, Sayegh V. New roentgenologic signs of carcinoma of the ureter. AJR. 1961;86(4):707–17.
160. Leder RA, Dunnick NR. Transitional cell carcinoma of the pelvicalices and ureter. AJR Am J Roentgenol. 1990; 155(4):713–22.
161. Chiu YS, Chiang HW, Huang CY, Tsai TJ. ARF after retrograde pyelography: a case report and literature review. Am J Kidney Dis. 2003;42(2):E13–6.
162. Hurley RM. Acute renal failure secondary to bilateral retrograde pyelography. Clinical Pediatrics. 1979;18(12):754–6.
163. Whalley DW, Ibels LS, Eckstein RP, Alexander JH, Smith RD. Acute tubular necrosis complicating bilateral retrograde pyelography. Aust N Z J Med. 1987;17(5):536–8.
164. Lytton B, Brooks MB, Spencer RP. Absorption of contrast material from the urinary tract during retrograde pyelography. J Urology. 1968;100(6):779–82.
165. Marshall WH Jr, Castellino RA. The urinary mucosal barrier in retrograde pyelography. The role of the ureteric mucosa. Radiology. 1970;97(1):5–7.
166. Castellino RA, Marshall WH Jr. The urinary mucosal barrier in retrograde pyelography: experimental findings and clinical implications. Radiology. 1970;95(2):403–9.
167. Weese DL, Greenberg HM, Zimmern PE. Contrast media reactions during voiding cystourethrography or retrograde pyelography. Urology. 1993;41(1):81–4.
168. Johenning PW. Reactions to contrast material during retrograde pyelography. Urology. 1980;16(4):442–4.
169. Miller KT, Moshyedi AC. Systemic reaction to contrast media during cystography. AJR Am J Roentgenol. 1995;164(6):1551.
170. Gaiser RR, Chua E. Anaphylactic/anaphylactoid reaction to contrast dye administered in the ureter. J Clin Anesth. 1993;5(6): 510–2.
171. Cohan RH, Leder RA, Ellis JH. Treatment of adverse reactions to radiographic contrast media in adults. Radiol Clin North Am. 1996;34(5):1055–76.
172. Chen GL, El-Gabry EA, Bagley DH. Surveillance of upper urinary tract transitional cell carcinoma: the role of ureteroscopy, retrograde pyelography, cytology and urinalysis. J Urol. 2000;164(6):1901–4.
173. Selzman AA, Spirnak JP. Iatrogenic ureteral injuries: a 20-year experience in treating 165 injuries. J Urol. 1996;155(3):878–81.
174. Armenakas NA, Pareek G, Fracchia JA. Iatrogenic bladder perforations: longterm followup of 65 patients. J Am Coll Surg. 2004;198(1):78–82.
175. Pansadoro V, Emiliozzi P. Iatrogenic prostatic urethral strictures: classification and endoscopic treatment. Urology. 1999;53(4):784–9.
176. Stormont TJ, Suman VJ, Oesterling JE. Newly diagnosed bulbar urethral strictures: etiology and outcome of various treatments. J Urol. 1993;150(5 Pt 2):1725–8.
177. Smith AD. Management of iatrogenic ureteral strictures after urological procedures. J Urol. 1988;140(6):1372–4.
178. Howards SS, Harrison JH. Retroperitoneal phlegmon. A fatal complication of retrograde pyelography. J Urology. 1973;109(1):92–3.
179. Ku JH, Lee SW, Jeon HG, Kim HH, Oh SJ. Percutaneous nephrostomy versus indwelling ureteral stents in the management of extrinsic ureteral obstruction in advanced malignancies: are there differences? Urology. 2004;64(5):895–9.
180. Mokhmalji H, Braun PM, Martinez Portillo FJ, Siegsmund M, Alken P, Kohrmann KU. Percutaneous nephrostomy versus ureteral stents for diversion of hydronephrosis caused by stones: a prospective, randomized clinical trial. J Urol. 2001;165(4): 1088–92.
181. Watson RA, Esposito M, Richter F, Irwin RJ Jr, Lang EK. Percutaneous nephrostomy as adjunct management in advanced upper urinary tract infection. Urology. 1999;54(2):234–9.
182. Pearle MS, Pierce HL, Miller GL, et al. Optimal method of urgent decompression of the collecting system for obstruction and infection due to ureteral calculi. J Urol. 1998;160(4):1260–4.

183. Thomsen HS. Pressures during retrograde pyelography. Acta Radiol Diagn. 1983;24(2):171–5.
184. Thomsen HS, Dorph S. Pyelorenal backflow during retrograde pyelography in adult patients. Scand J Urol Nephrol. 1981;15(1):65–8.
185. Thomsen HS, Larsen S. Intrarenal backflow during retrograde pyelography with graded intrapelvic pressure. a pathoanatomic study. Acta Pathol Microbiol Immunol Scand [A]. 1983;91(4):245–52.
186. Bidgood WD Jr, Cuttino JT Jr, Clark RL, Volberg FM. Pyelovenous and pyelolymphatic backflow during retrograde pyelography in renal vein thrombosis. Invest Radiol. 1981;16(1):13–9.
187. Murayama S, Shimoda Y, Kishikawa T. Pyelovenous backflow in left renal vein hypertension: case report. Radiat Med. 1989;7(2):55–7.
188. Helin I, Okmian L, Olin T. Renal blood flow and function at elevated ureteric pressure. An experimental study in the pig. Scand J Urol Nephrol. 1975;28 Suppl:53–69.
189. McAninch LN, Mostafa HM. Pyelocancerous backflow. A diagnostic radiological sign for renal cell carcinoma. J Urol. 1971;105(4):491.
190. Copeland JS, Schellhammer PF, Devine CJ Jr. Pyelocancerous backflow: a radiologic finding in renal malignancy. J Urol. 1976;115(2):214–5.
191. Thomsen HS, Dorph S. Pyelorenal backflow during retrograde pyelography after renal transplantation. Scand J Urol Nephrol. 1978;12(2):175–9.
192. Thomsen HS. Intrarenal backflow during retrograde pyelography following kidney transplantation. Acta Radiol Diagn. 1984;25(2):113–20.
193. Thomsen HS, Talner LB, Higgins CB. Intrarenal backflow during retrograde pyelography with graded intrapelvic pressure. A radiologic study. Invest Radiol. 1982;17(6):593–603.
194. Thomsen HS, Dorph S, Olsen S. Pyelorenal backflow in normal and ischemic rabbit kidneys. Invest Radiol. 1981;16(3):206–14.
195. Thomsen HS, Larsen S, Talner LB. Pyelorenal backflow during retrograde pyelography in normal and ischemic porcine kidneys. A radiologic and pathoanatomic study. Eur Urol. 1982;8(5):291–7.
196. Friedenberg RM, Moorehouse H, Gade M. Urinomas secondary to pyelosinus backflow. Urol Radiol. 1983;5(1):23–9.
197. Ihara H, Ihara Y, Sagawa S, Takaha M, Sonoda T. Pyelosinus backflow: a case with an unusual pyelographic appearance. Urol Radiol. 1980;2(4):263–4.
198. Titton RL, Gervais DA, Hahn PF, Harisinghani MG, Arellano RS, Mueller PR. Urine leaks and urinomas: diagnosis and imaging-guided intervention. Radiographics. 2003;23(5):1133–47.
199. Burns JE. Thorium, a new agent for pyelography, preliminary report. JAMA. 1915;64:2126–7.
200. Oyen RH, Gielen JL, Van Poppel HP, et al. Renal thorium deposition associated with transitional cell carcinoma: radiologic demonstration in two patients. Radiology. 1988;169(3):705–7.
201. Griffiths MH, Thomas DP, Xipell JM, Hope RN. Thorotrast-induced bilateral carcinoma of the kidney. Pathology. 1977;9(1):43–8.
202. Kauzlaric D, Barmeir E, Luscieti P, Binek J, Ramelli F, Petrovic M. Renal carcinoma after retrograde pyelography with Thorotrast. AJR Am J Roentgenol. 1987;148(5):897–8.
203. Mihatsch MJ, Rutishauser G. Thorotrast induced transitional cell carcinoma in a residual ureter after nephrectomy. Cancer. 1973;32(6):1346–9.
204. Wenz W. Tumors of the kidney following retrograde pyelography with colloidal thorium dioxide. Ann N Y Acad Sci. 1967;145(3):806–10.
205. Kapandji M. Ponction de bassinet et radiomanometrie meato-uretero-pyelocalicielle. Bull Mem Soc Med Hop Paris M. 1949;849:21–2.
206. Goodwin WE, Casey WC, Woolf W. Percutaneous trocar (needle) nephrostomy in hydronephrosis. JAMA. 1955;157(11):891–4.
207. Casey WC, Goodwin WE. Percutaneous antegrade pyelography and hydronephrosis. J Urol. 1955;74(1):164–73.
208. Weens HS, Florence TJ. The diagnosis of hydronephrosis by percutaneous renal puncture. J Urol. 1954;72(4):589–95.
209. Wickbom I. Pyelography after direct puncture of the renal pelvis. Acta Radiol. 1954;41:505.
210. Fritzsche P. Antegrade pyelography: therapeutic applications. Radiol Clin North Am. 1986;24(4):573–86.
211. Pedersen JF. Percutaneous nephrostomy guided by ultrasound. J Urol. 1974;112(2):157–9.
212. Hellsten S, Hildell J, Link D, Ulmsten U. Percutaneous nephrostomy. Aspects on applications and technique. Eur Urol. 1978;4(4):282–7.
213. Zegel HG, Pollack HM, Banner MC, et al. Percutaneous nephrostomy: comparison of sonographic and fluoroscopic guidance. AJR Am J Roentgenol. 1981;137(5):925–7.
214. Hay MS, Elyaderani MK, Belis JA. Percutaneous approach to the renal pelvis: combined use of ultrasonography and fluoroscopy. South Med J. 1981;74(1):31–3.
215. Myers RP. Brodel's line. Surg Gynecol Obstet. 1971;132(3): 424–6.
216. Dyer RB, Regan JD, Kavanagh PV, Khatod EG, Chen MY, Zagoria RJ. Percutaneous nephrostomy with extensions of the technique: step by step. Radiographics. 2002;22(3):503–25.
217. Zagoria RJ, Dyer RB. Do's and don't's of percutaneous nephrostomy. Acad Radiol. 1999;6(6):370–7.
218. Boon JM, Shinners B, Meiring JH. Variations of the position of the colon as applied to percutaneous nephrostomy. Surg Radiol Anat. 2001;23(6):421–5.
219. O'Donnell A, Schoenberger C, Weiner J, Tsou E. Pulmonary complications of percutaneous nephrostomy and kidney stone extraction. South Med J. 1988;81(8):1002–5.
220. Radecka E, Brehmer M, Holmgren K, Magnusson A. Complications associated with percutaneous nephrolithotripsy: supra- versus subcostal access. A retrospective study. Acta Radiol. 2003;44(4):447–51.
221. Ostendorf N, van Ahlen H, Hertle L. Simple reinforcement for thin nephrostomy catheters. J Urol. 1998;159(2):485–6.
222. Watson G. Problems with double-J stents and nephrostomy tubes. J Endourol. 1997;11(6):413–7.
223. Paul EM, Marcovich R, Lee BR, Smith AD. Choosing the ideal nephrostomy tube. BJU Int. 2003;92(7):672–7.
224. Lewis S, Patel U. Major complications after percutaneous nephrostomy-lessons from a department audit. Clin Radiol. 2004;59(2):171–9.
225. Sim LS, Tan BS, Yip SK, et al. Single centre review of radiologically-guided percutaneous nephrostomies: a report of 273 procedures. Ann Acad Med Singapore. 2002;31(1):76–80.
226. Lee WJ, Mond DJ, Patel M, Pillari GP. Emergency percutaneous nephrostomy: technical success based on level of operator experience. J Vasc Interv Radiol. 1994;5(2):327–30.
227. Lee WJ, Patel U, Patel S, Pillari GP. Emergency percutaneous nephrostomy: results and complications. J Vasc Interv Radiol. 1994;5(1):135–9.
228. Sengupta S, Harewood L. Transitional cell carcinoma growing along an indwelling nephrostomy tube track. Br J Urol. 1998;82(4):591.
229. Huang A, Low RK, deVere White R. Nephrostomy tract tumor seeding following percutaneous manipulation of a ureteral carcinoma. J Urol. 1995;153(3 Pt 2):1041–2.

230. Gerber GS, Lyon ES. Endourological management of upper tract urothelial tumors. J Urol. 1993;150(1):2–7.
231. Thalmann GN, Markwalder R, Walter B, Studer UE. Long-term experience with bacillus Calmette-Guerin therapy of upper urinary tract transitional cell carcinoma in patients not eligible for surgery. J Urol. 2002;168(4 Pt 1):1381–5.
232. Guz B, Streem SB, Novick AC, et al. Role of percutaneous nephrostomy in patients with upper urinary tract transitional cell carcinoma. Urology. 1991;37(4):331–6.
233. Goel MC, Mahendra V, Roberts JG. Percutaneous management of renal pelvic urothelial tumors: long-term followup. J Urol. 2003;169(3):925–9; discussion 929–30.
234. Clark PE, Streem SB, Geisinger MA. 13-year experience with percutaneous management of upper tract transitional cell carcinoma. J Urol. 1999;161(3):772–5; discussion 775–6.
235. Elliott DS, Segura JW, Lightner D, Patterson DE, Blute ML. Is nephroureterectomy necessary in all cases of upper tract transitional cell carcinoma? Long-term results of conservative endourologic management of upper tract transitional cell carcinoma in individuals with a normal contralateral kidney. Urology. 2001;58(2):174–8.
236. Shepherd SF, Patel A, Bidmead AM, Kellett MJ, Woodhouse CR, Dearnaley DP. Nephrostomy track brachytherapy following percutaneous resection of transitional cell carcinoma of the renal pelvis. Clin Oncol (R Coll Radiol). 1995;7(6):385–7.
237. Whitaker RH. Pressure-controlled nephrostography. Eur Urol. 1977;3(3):145–9.
238. Witherow RO, Whitaker RH. The predictive accuracy of antegrade pressure flow studies in equivocal upper tract obstruction. Br J Urol. 1981;53(6):496–9.
239. Wahlin N, Magnusson A, Persson AE, Lackgren G, Stenberg A. Pressure flow measurement of hydronephrosis in children: a new approach to definition and quantification of obstruction. J Urol. 2001;166(5):1842–7.
240. Gonzalez R, Chiou R. The diagnosis of upper urinary tract obstruction in children: comparison of diuresis renography and pressure flow studies. J Urol. 1985;133(4):646–9.
241. Jakobsen H, Nordling J, Munck O, Iversen P, Nielsen SL, Holm HH. Sensitivity of 131I-hippuran diuresis renography and pressure flow study (Whitaker test) in upper urinary tract obstruction. Urol Int. 1988;43(2):89–92.
242. Kashi SH, Irving HC, Sadek SA. Does the Whitaker test add to antegrade pyelography in the investigation of collecting system dilatation in renal allografts? Br J Radiol. 1993;66(790):877–81.
243. Yokogi H, Wada Y, Mizutani M, Igawa M, Ishibe T. Bacillus Calmette-Guerin perfusion therapy for carcinoma in situ of the upper urinary tract. Br J Urol. 1996;77(5):676–9.
244. Patel A, Soonawalla P, Shepherd SF, Dearnaley DP, Kellett MJ, Woodhouse CR. Long-term outcome after percutaneous treatment of transitional cell carcinoma of the renal pelvis. J Urol. 1996;155(3):868–74.
245. See WA. Continuous antegrade infusion of adriamycin as adjuvant therapy for upper tract urothelial malignancies. Urology. 2000;56(2):216–22.
246. Sacha K, Szewczyk W, Bar K. Massive haemorrhage presenting as a complication after percutaneous nephrolithotomy (PCNL). Int Urol Nephrol. 1996;28(3):315–8.
247. Martin X, Murat FJ, Feitosa LC, et al. Severe bleeding after nephrolithotomy: results of hyperselective embolization. Eur Urol. 2000;37(2):136–9.
248. Davidoff R, Bellman GC. Influence of technique of percutaneous tract creation on incidence of renal hemorrhage. J Urol. 1997;157(4):1229–31.
249. Kessaris DN, Bellman GC, Pardalidis NP, Smith AG. Management of hemorrhage after percutaneous renal surgery. J Urol. 1995;153(3 Pt 1):604–8.
250. Lee WJ, Smith AD, Cubelli V, et al. Complications of percutaneous nephrolithotomy. AJR Am J Roentgenol. 1987;148(1):177–80.
251. Stoller ML, Wolf JS Jr, St Lezin MA. Estimated blood loss and transfusion rates associated with percutaneous nephrolithotomy. J Urol. 1994;152(6 Pt 1):1977–81.
252. Kukreja R, Desai M, Patel S, Bapat S. Factors affecting blood loss during percutaneous nephrolithotomy: prospective study. J Endourol. 2004;18(8):715–22.
253. Routh WD, Tatum CM, Lawdahl RB, Rosch J, Keller FS. Tube tamponade: potential pitfall in angiography of arterial hemorrhage associated with percutaneous drainage catheters. Radiology. 1990;174(3 Pt 2):945–9.
254. Kaye KW, Clayman RV. Tamponade nephrostomy catheter for percutaneous nephrostolithotomy. Urology. 1986;27(5):441–5.
255. Jou YC, Cheng MC, Sheen JH, Lin CT, Chen PC. Electrocauterization of bleeding points for percutaneous nephrolithotomy. Urology. 2004;64(3):443–6; discussion 446–7.
256. Jou YC, Cheng MC, Sheen JH, Lin CT, Chen PC. Cauterization of access tract for nephrostomy tube-free percutaneous nephrolithotomy. J Endourol. 2004;18(6):547–9.
257. Mikhail AA, Kaptein JS, Bellman GC. Use of fibrin glue in percutaneous nephrolithotomy. Urology. 2003;61(5):910–4; discussion 914.
258. Pfab R, Ascherl R, Blumel G, Hartung R. Local hemostasis of nephrostomy tract with fibrin adhesive sealing in percutaneous nephrolithotomy. Eur Urol. 1987;13(1–2):118–21.
259. Orzel JA, Coldwell DM, Eskridge JM. Superselective embolization for renal hemorrhage with a new coaxial catheter and steerable guidewire. Cardiovasc Intervent Radiol. 1988;11(6):343–5.
260. Peene P, Wilms G, Baert AL. Embolization of iatrogenic renal hemorrhage following percutaneous nephrostomy. Urol Radiol. 1990;12(2):84–7.
261. Ueda J, Furukawa T, Takahashi S, Miyake O, Itatani H, Araki Y. Arterial embolization to control renal hemorrhage in patients with percutaneous nephrostomy. Abdom Imaging. 1996;21(4):361–3.
262. Gupta M, Bellman GC, Smith AD. Massive hemorrhage from renal vein injury during percutaneous renal surgery: endourological management. J Urol. 1997;157(3):795–7.
263. Cowan NC, Traill ZC, Phillips AJ, Gleeson FV. Direct percutaneous transrenal embolization for renal artery injury following percutaneous nephrostomy. Br J Radiol. 1998;71(851):1199–201.
264. Beaujeux R, Saussine C, al-Fakir A, et al. Superselective endo-vascular treatment of renal vascular lesions. J Urol. 1995;153(1):14–7.
265. Kernohan RM, Johnston LC, Donaldson RA. Bleeding following percutaneous nephrolithotomy resulting in loss of the kidney. Br J Urol. 1990;65(6):657–8.
266. Dorffner R, Thurnher S, Prokesch R, et al. Embolization of iatrogenic vascular injuries of renal transplants: immediate and follow-up results. Cardiovasc Intervent Radiol. 1998;21(2):129–34.
267. Demirbas O, Batyraliev T, Eksi Z, Pershukov I. Femoral pseudoaneurysm due to diagnostic or interventional angiographic procedures. Angiology. 2005;56(5):553–6.
268. Ferguson JD, Whatling PJ, Martin V, Walton J, Banning AP. Ultrasound guided percutaneous thrombin injection of iatrogenic femoral artery pseudoaneurysms after coronary angiography and intervention. Heart. 2001;85(4):E5.
269. Pejic R. Iatrogenic arteriovenous fistula of the profunda femoris artery/vein: a case report. Indiana Med. 1990;83(2):118–20.
270. Marsan RE, McDonald V, Ramamurthy S. Iatrogenic femoral arteriovenous fistula. Cardiovasc Intervent Radiol. 1990;13(5):314–6.
271. Sakamoto I, Hayashi K, Matsunaga N, et al. Aortic dissection caused by angiographic procedures. Radiology. 1994;191(2):467–71.

272. Gorog DA, Watkinson A, Lipkin DP. Treatment of iatrogenic aortic dissection by percutaneous stent placement. J Invasive Cardiol. 2003;15(2):84–5.
273. Sharma PV, Babu SC, Shah PM, Nassoura ZE. Changing patterns of atheroembolism. Cardiovasc Surg. 1996;4(5):573–9.
274. Cronan JJ, Dorfman GS, Amis ES, Denny DF Jr. Retroperitoneal hemorrhage after percutaneous nephrostomy. AJR Am J Roentgenol. 1985;144(4):801–3.
275. Merine D, Fishman EK. Perirenal hematoma following catheter removal. An unusual complication of percutaneous nephrostomy. Clin Imaging. 1989;13(1):74–6.
276. Hergesell O, Felten H, Andrassy K, Kuhn K, Ritz E. Safety of ultrasound-guided percutaneous renal biopsy-retrospective analysis of 1090 consecutive cases. Nephrol Dial Transplant. 1998;13(4):975–7.
277. Merkus JW, Zeebregts CJ, Hoitsma AJ, van Asten WN, Koene RA, Skotnicki SH. High incidence of arteriovenous fistula after biopsy of kidney allografts. Br J Surg. 1993;80(3):310–2.
278. Hubsch P, Schurawitzki H, Traindl O, Karnel F. Renal allograft arteriovenous fistula due to needle biopsy with late onset of symptoms—diagnosis and treatment. Nephron. 1991;59(3):482–5.
279. Brandenburg VM, Frank RD, Riehl J. Color-coded duplex sonography study of arteriovenous fistulae and pseudoaneurysms complicating percutaneous renal allograft biopsy. Clin Nephrol. 2002;58(6):398–404.
280. Mansy H, Khalil A, Bafaqeeh M, et al. Transplant nephrectomy for a large AV fistula following renal biopsy. Nephron. 1995;71(4):481–2.
281. deSouza NM, Reidy JF, Koffman CG. Arteriovenous fistulas complicating biopsy of renal allografts: treatment of bleeding with superselective embolization. AJR Am J Roentgenol. 1991;156(3):507–10.
282. Gerspach JM, Bellman GC, Stoller ML, Fugelso P. Conservative management of colon injury following percutaneous renal surgery. Urology. 1997;49(6):831–6.
283. Hussain M, Hamid R, Arya M, Peters JL, Kellett MJ, Philip T. Management of colonic injury following percutaneous nephrolithotomy. Int J Clin Pract. 2003;57(6):549–50.
284. Vallancien G, Capdeville R, Veillon B, Charton M, Brisset JM. Colonic perforation during percutaneous nephrolithotomy. J Urol. 1985;134(6):1185–7.
285. Wolf JS Jr. Management of intraoperatively diagnosed colonic injury during percutaneous nephrostolithotomy. Tech Urol. 1998;4(3):160–4.
286. Robert M, Maubon A, Roux JO, Rouanet JP, Navratil H. Direct percutaneous approach to the upper pole of the kidney: MRI anatomy with assessment of the visceral risk. J Endourol. 1999;13(1):17–20.
287. Hopper KD, Yakes WF. The posterior intercostal approach for percutaneous renal procedures: risk of puncturing the lung, spleen, and liver as determined by CT. AJR Am J Roentgenol. 1990;154(1):115–7.
288. Kondas J, Szentgyorgyi E, Vaczi L, Kiss A. Splenic injury: a rare complication of percutaneous nephrolithotomy. Int Urol Nephrol. 1994;26(4):399–404.
289. Hopper KD, Chantelois AE. The retrorenal spleen. Implications for percutaneous left renal invasive procedures. Invest Radiol. 1989;24(8):592–5.
290. Gouze VA, Breslow MJ. Hydrothorax as a complication of percutaneous access to the renal pelvis. Anesth Analg. 1996;83(3):652–3.
291. Radecka E, Magnusson A. Complications associated with percutaneous nephrostomies. A retrospective study. Acta Radiol. 2004;45(2):184–8.
292. Gupta R, Kumar A, Kapoor R, Srivastava A, Mandhani A. Prospective evaluation of safety and efficacy of the supracostal approach for percutaneous nephrolithotomy. BJU Int. 2002;90(9):809–13.
293. Forsyth MJ, Fuchs EF. The supracostal approach for percutaneous nephrostolithotomy. J Urol. 1987;137(2):197–8.

Chapter 28

Positron Emission Tomography (PET) in Germ Cell Tumors (GCT)

M. De Santis, A. Maj-Hes, and M. Bachner

Introduction

Both the treatment and outcome of germ cell tumors (GCT) have changed with the implementation of cisplatin-based chemotherapy. High cure rates even in advanced tumor stages provide a unique scenario for young cancer survivors who look for optimal patient management with minimal acute and long-term morbidity and toxicity. Non-invasive staging tools like serum tumor marker assays and imaging studies such as computed tomography (CT) both made substantial contributions to this goal. Improved staging and response evaluation help to avoid unnecessary overtreatment by risk-adapted approaches precisely tailored to the individual patient.

However, conventional staging techniques still are prone to considerable over- and understaging attributable to their sensitivity and specificity [1–3].

Positron emission tomography (PET) is a more recent addition to the battery of clinical diagnostic tools. With this imaging technique, a non-invasive method for determining regional metabolic processes has become available. The use of PET in oncology is based on the well-founded assumption that the visualization of metabolic changes often precedes measurable morphologic alterations in neoplastic tissue [4–7]. Thus PET has added a new dimension, i.e., metabolic imaging, to current anatomy-derived imaging techniques.

M. De Santis (✉)
3rd Medical Department - Center for Oncology and Hematology
Ludwig Boltzmann-Institute for Applied Cancer Research Vienna (LBI-ACR VIEnna)
Kaiser Franz Josef - Spital der Stadt Wien and
Applied Cancer Research Institution for Translational Research Vienna (ACR-ITR VIEnna)/CEADDP
Kundratstrasse 3, A-1100 Vienna, Austria
maria.desantis@wienkav.at

Physics

The principle underlying positron emission tomography (PET) is that when binding to electrons, positrons from positron-emitting radioisotopes release annihilation gamma rays. These consist of two photons of 511 keV each separating in diametrical directions and are detected by a ring of detectors with opposed scintillation crystals, which recognize coincident radiation events. PET produces both dynamic data like the movements in time of the injected tracer and its distribution in a circumscribed area and static data such as those obtained by whole body scans, which image the structures of interest in three dimensions (coronal, transverse, and sagittal) and are generally used for evaluating cancer patients. *S*tandard tracer *u*ptake *v*alues (SUVs) are being calculated in an attempt to quantify the intensity of local tracer uptake in the region of interest and to obtain results, which are easily compared with the results at another point in the course of the disease:

SUV = decay corrected maximal region of interest activity/injected dose / body weight

However, the usefulness and the reproducibility of SUVs compared to visual interpretation by an experienced nuclear physicist have repeatedly been questioned [8, 9].

Currently, the most sophisticated standard scanners, i.e., full-ring tomograph scanners [10], have a resolution of 4–5 mm. They detect volumes with positive tracer uptake down to 8–10 mL. The technology involved is complex and the costs incurred are high.

Tracers in GCT

In oncology, 2-^{18}fluoro-2-deoxy-D-glucose (FDG) is currently the most widely used tracer, because it selectively accumulates in cancer cells. On account of the regionally increased blood flow and the elevated activity of glucose transporters (GluT1) and intracellular hexokinase, cancer cells are avid glucose seekers. ^{18}F substitution at the C2

J.J.M.C.H. de la Rosette et al. (eds.), *Imaging in Oncological Urology*,
DOI 10.1007/978-1-84628-759-6_28,

of the glucose structure turns ^{18}FDG-6-phosphate into a polar molecule, which cannot be further metabolized and, as cancer cells contain little glucose-6-phosphatase, is trapped in them. These mechanisms contribute to distinguishing active tumor from non-neoplastic cells by its increased tracer uptake [11–13].

A few other tracers have been under investigation for GCTs, among them L-(1-carbon-11)tyrosine [14], which has, however, not been found to be suited for evaluating residual masses in GCT.

The following physiologic issues and limitations of FDG PET should be considered before clinical decision-making with the help of FDG PET:

Physiologic FDG Uptake

FDG also actively accumulates in normal tissues of the brain, the myocardium, the liver, the smooth muscles, and the bone marrow and is eliminated along renal and urinary pathways. Three-dimensional imaging and iterative reconstruction help to differentiate these superimposed structures from neoplastic tissue [15].

False Positive FDG PET Results

High FDG uptake is not totally tumor specific. It is well known that inflammatory and granulomatous tissue such as sarcoidosis show extensive tracer uptake caused by elevated macrophage activity [16–18]. This is also true for inflammatory reactions up to several months after irradiation [19, 20]. Active [^{18}F]FDG uptake by phagocytes within abscesses or by granulation tissue surrounding abscesses causes false positive results, whereas chemically sterile abscesses do not accumulate FDG [4]. Macrophage accumulation due to resorption of necrotic post-treatment tumor tissue will cause false positive FDG PET studies. Most importantly, there may be a metabolic flare within the first days after chemotherapy. Therefore, PET should not be performed too early in germ cell residual tumors after chemotherapy, i.e., within 2–4 weeks post-chemotherapy [17, 21, 22].

False Negative FDG PET Results

The timing of PET studies is of utmost importance. FDG uptake by neoplastic tissue may be reduced within 2 weeks of exposure to cytostatics [16]. This phenomenon is tumor- and treatment specific. In gastrointestinal stroma tumors (GIST), for instance, reduced uptake (true negative result) after exposure to imatinib mesylate has been described after only 24 h [23].

The size of the lesions to be evaluated is important as well. Due to the limited resolution we do not expect FDG PET to be positive in low-volume disease, e.g., lesions < 5 mm. But PET may detect extremely active lesions between 5 and 10 mm in size [5, 24–30].

PET for Non-invasive Tumor Staging

Consistent prospective data have established the clinical role of FDG PET in oncology particularly for staging non-small-cell lung cancer, colorectal cancer, and melanoma, for evaluating single pulmonary lesions, for detecting liver metastases, and for staging cancers with unknown primaries [11, 13, 31–35]. In Non-Hodgkin's lymphoma and Hodgkin's disease PET has become crucial for staging, treatment evaluation, early detection of relapse, and most recently for distinguishing aggressive and indolent disease [36–41].

FDG PET in Germ Cell Tumors (GCT)

Germ cell tumors as well as their secondaries are generally characterized by a high FDG uptake. Pure seminomas accumulate even more FDG than non-seminomatous lesions [5, 16, 42]. This very fact led numerous research teams to investigate the clinical role of FDG PET in GCT.

The following chapter will summarize the current state-of-the-art knowledge about the use of PET in different clinical situations during the treatment of germ cell tumors. Evidence derived from published trials and its consequences will be discussed. The pros and cons of PET scanning will be put into the context of crucial points in clinical decision-making. These include

- Staging at presentation
- Response evaluation
- Management of relapse

Staging at Presentation

Non-seminomatous and Seminomatous Germ Cell Tumors (NSGCT and SGCT)

Staging of GCT at presentation in clinical stages I and II with CT scans has a limited accuracy of about 70% [2, 30, 43, 44]. After staging by CT 20–30% of clinical stage II patients turn out to be stage I pathologically. On the other hand, CT underestimates the pathologic stage in up to 30% of patients

[43, 45]. The smaller the lymph nodes the higher the sensitivity, but the lower the specificity [2, 46, 47].

The role of FDG PET for initial staging in unselected NSGCT and SGCT patients was the subject of investigation in several trials [5, 16, 22, 24–29], two of which [22, 29] reported a higher sensitivity and a higher negative predictive value (NPV) for PET versus CT. The specificities of the two methods were comparable. No clinical consequences were drawn. Recently, a German group investigated the sensitivity, specificity, and accuracy of FDG PET in stage I/II NSGCT patients scheduled for primary retroperitoneal lymph node dissection (RPLND). There was no difference between CT and FDG PET in terms of false negative results, especially in small lesions [30].

In most of the studies PET failed to detect small (< 1 or < 0.5 cm) retroperitoneal lymph nodes [5, 24–30] and mature teratomas [24, 28]. One of the positive PET scans in one trial was attributable to sarcoidosis [16]. None of the trials unequivocally established a benefit of PET versus conventional staging with tumor markers and CT at presentation.

Summary

To date there is no proof of a benefit of PET for staging at presentation.

Clinical Stage I Non-seminomatous Germ Cell Tumors (NSGCT)

After orchiectomy about 30% of clinical stage I NSGCT patients staged with conventional techniques like (spiral-) CT scans will relapse within the first 2 years after the diagnosis.

The most accurate staging technique for the retroperitoneum, i.e., retroperitoneal lymphadenectomy, is very invasive for just a staging procedure, and its cure rate is no better than 10–15% [1, 47]. Systematic adjuvant short-term chemotherapy of high-risk clinical stage I patients in terms of risk-adapted treatment [48] is tantamount to overtreatment in as many as 50% of cases. Therefore, improved staging tools would be of utmost importance in clinical stage I GCT.

Three of four trials examining FDG PET for staging clinical stage I NSGCT patients with no more than a total of 27 patients correlated PET data with histopathology data obtained from subsequent (RPLND) [24, 27, 28]. In all three trials PET failed to improve clinical staging. Of 22 negative PET scans, seven proved to be false negative (NPV 68%): in six patients the histologically positive lymph nodes were smaller than 0.5 cm and in the remaining patient PET failed to detect a mature teratoma. PET (sensitivity 42%) correctly identified no more than 5 out of 12 metastasizing patients [24, 27, 28]. In the fourth study by Lassen et al. [49], PET data of 46 patients were compared to clinical follow-up data collected during surveillance. In this prospective trial, by contrast, 7 out of 10 relapses were correctly predicted (sensitivity 70%) and no more than 3 out of 39 negative PET scans proved to be false negative (NPV 92%). This prompted the authors to conclude that FDG PET had improved clinical staging in their patients. A CT review later on classified two patients to be stage II, who finally had to be removed from the analysis. After all, the sensitivity of FDG PET in this study fell to 50% [50]. Based on the initial results of this trial [49], the Medical Research Council initiated a prospective large-scale trial to investigate the role of FDG PET in high-risk clinical stage I NSGCT. PET-positive patients enrolled in this trial were subjected to adjuvant chemotherapy, while those with negative PET scans were put on surveillance. The study was closed early in 2005, after 33 out of 88 PET-negative patients had relapsed, with a 1 year relapse-free rate of 63.3% instead of the expected 2-year relapse-free rate of $> 90\%$ [51].

Summary

FDG PET has no role for staging or early detection of micrometastases in clinical stage I NSGCT.

Clinical Stage I Seminoma

Clinical stage I seminoma patients overall run a relapse risk of 18% [52] without further adjuvant treatment. Patients are usually offered adjuvant standard radiation therapy or are put on a surveillance protocol. Adjuvant chemotherapy with carboplatin has become a third option [53, 54], because randomized data still lack sufficient follow-up time and peer-reviewed publication. Any kind of adjuvant treatment in clinical stage I seminoma causes an overtreatment rate of about 80%.

So far, no scientific evidence is available for a positive role of PET in this clinical setting. Albers and Müller-Matheis [24, 27] described 31 clinical stage I seminoma patients, all of them with negative PET scans. But as all of them had undergone adjuvant radiotherapy, there is no way of telling whether the PET data was correct or not.

The role of PET in an adjuvant setting should be analyzed in patients under surveillance.

Summary

FDG PET has no advantage over CT in staging clinical stage I SGCT.

Clinical Stage II Disease/NSGCT

In clinical stage II, particularly in stage IIa disease, pathologic staging with RPLND shows that in up to 25% of cases patients are overstaged by CT [43]. FDG PET data for this clinical situation are contradictory: in a study by Albers et al. [24] CT staging was false positive in four out of nine clinical stage II NSGCT patients, while PET correctly staged all nine patients. Of the seven patients with clinical stage II disease contributed by Spermon et al. [28], all were correctly staged by CT, while PET failed to detect metastatic embryonic carcinoma in a retroperitoneal lymph node 1.2 cm in size and metastatic mature teratoma in another.

Summary

There is no evidence-based support for the use of FDG PET in stage II NSCGT.

Response Evaluation

Post-chemotherapy Residual Masses in NSGCT

After completion of cisplatin-based chemotherapy, one quarter to one third of all patients with metastases of NSGCT present with residual masses, although their tumor marker levels have returned to normal (marker-negative partial remissions; PRm-). These patients are candidates for residual tumor surgery. Multiple series of histological studies after RPLND show that only 40–45% of these residuals consist of necrotic/fibrotic tissue, while 10–20% harbor viable tumor and 30–45% mature teratoma [55, 56]. The latter two, viable tumor and mature teratoma, are the source of recurrences and therefore have to be removed. Complete resection of all residual NSGCT lesions is the only way of curing this group of patients [57, 58].

However, resection of mere necrosis/fibrosis only does not offer any therapeutic benefits. Neither retrospective trials nor predictive models [59] based on regression analyses have so far reliably predicted the histology of the residual masses. Therefore, several authors [16, 17, 27–29, 42, 60–63] evaluated FDG PET for its predictive potential in this clinical setting. Four of them were prospective trials [17, 27, 42, 61].

The authors unequivocally found that PET predicted viable tumor within the residual lesions with a high measure of diagnostic accuracy, except in very small residuals. Unfortunately, FDG PET failed to distinguish between mature teratoma and necrosis/fibrosis, because both accumulate very little or no FDG. Therefore, FDG PET does not help in deciding for or against surgery. Based on kinetic modeling, only Sugawara et al. [63] reported differences in the kinetic rate constants of FDG uptake between mature teratoma and necrosis/fibrosis, albeit in no more than six patients.

The German multicenter trial, first presented as an abstract in 2006, showed an accuracy of only 57% for FDG PET for predicting vital tumor and teratoma in 141 patients with post-chemotherapy residual tumors. There was also a high rate of false positive results. Interestingly, the PET scans had been performed at an average of only 8.5 days after chemotherapy [30].

The studies quoted provided two important messages for the proper use and interpretation of PET in post-chemotherapy patients: (1) In some of them [16, 17, 27–29] inflammatory reactions with abundant macrophages accompanying tumor necrosis seen histologically were the most common cause of false positive PET scans. (2) FDG PET studies done shortly after chemotherapy (within less than 2 weeks) may be false negative because of a putative suppression of tumor cell metabolic activity regardless of their final treatment response [16]. Both of these observations suggest that an interval of several weeks post-chemotherapy should be allowed for PET scans.

Summary

Current evidence does not support the use of FDG PET for post-chemotherapy evaluation of NSGCT lesions.

Post-chemotherapy Residual Masses in SGCT

Residual lesions after chemotherapy of bulky SGCT are expected to be present in 50–75% of patients. Overall, less than 20% of the resected residual masses harbor viable tumor. Therefore, the management of seminoma residuals is controversial. Trying to find risk factors for the presence of viable tumor within the residual lesions, some authors found that the likelihood rose with the residual tumor size [64, 65]. The cut-off was drawn at a size of 3 cm.

The pronounced desmoplastic reaction of the tissue surrounding residual seminoma masses makes their resection technically demanding. Consequently, some authors prefer surveillance and reserve surgery for patients with progressive lesions [66], while others only resect lesions larger than 3 cm in diameter [65]. The advantage of FDG PET in SGCT compared to its use in NSGCT is that the presence of mature teratoma is extremely rare in SGCTs [65]. FDG PET, on the other hand, reliably differentiates viable tumor from necrosis/fibrosis in residual NSGCT. Therefore, two research groups examined seminoma residuals with FDG

PET in prospective trials comparing the results with histologic data or the clinical outcome.

In the single-center Indiana University study [67], only 1 out of 29 patients undergoing PET scanning at arbitrary intervals post-chemotherapy was PET-positive. The authors concluded that FDG PET was not helpful in distinguishing necrosis from viable seminoma, because it was false positive in one and false negative in five cases. In the Austrian–German prospective multicenter trial, by contrast, an interval of at least 4 weeks post-chemotherapy was mandatory for PET scanning. Preliminary data from the first 37 PET scans showed the specificity and the positive predictive value (PPV) to be 100% at a sensitivity of 89% and a NPV of 97% [64]. The discrepancies between these data and those found in the Indiana University study prompted the Austrian–German researchers to continue the trial and to expand it to 51 patients with post-chemotherapy residual masses and 56 FDG PET scans: All residual lesions $>$ 3 cm and 95% of those $\leq$ 3 cm were correctly predicted by FDG PET. The specificity, sensitivity, PPV, and NPV of FDG PET was 100, 80, 100, and 96%, respectively (Fig. 28.1). This is clearly superior to CT. The authors concluded that FDG PET was the best predictor of viable residual tumor in post-chemotherapy seminoma residuals and should be used as a standard tool for clinical decision-making in this patient group. The main advantage of using FDG PET in this clinical setting is that, in patients with residual lesions $>$ 3 cm, even in very large lesions, surgery can be omitted safely, if PET scans are negative. PET-positive residual lesions, according to this data set, must be regarded as harboring viable tumor and should be resected, if technically possible [68].

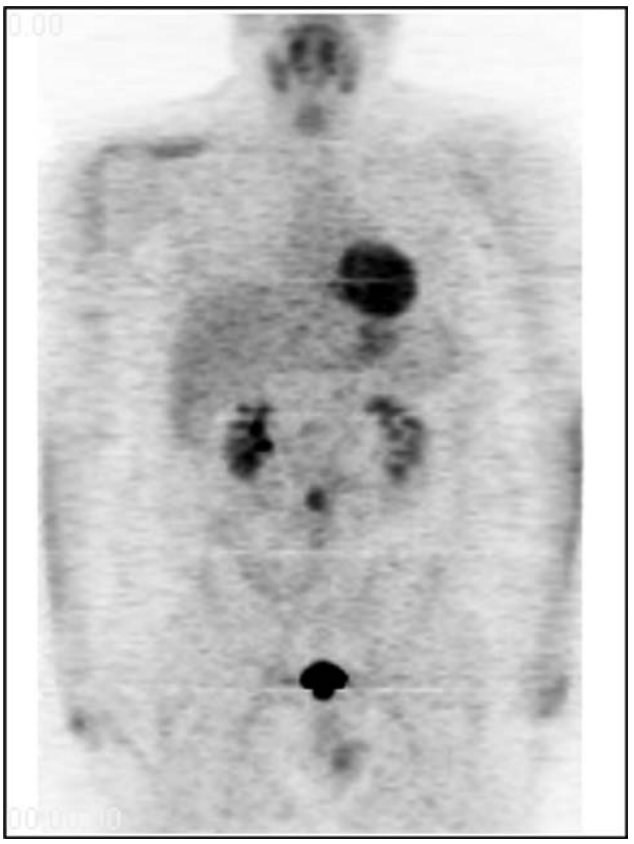

Fig. 28.1 FDG PET 6 weeks after chemotherapy for stage IIC SGCT. Histologically proven true positive residual lesion

Summary

FDG PET combined with CT studies for the evaluation of pure seminoma residuals can be regarded as a standard tool for clinical decision-making.

Early Prediction of Treatment Response to Salvage Chemotherapy

In some tumor entities FDG PET proved to be valuable for predicting treatment response non-invasively at an early point in time [23, 41, 69–71]. For first-line chemotherapy of germ cell tumors with a clear standard treatment and excellent cure rates, early response evaluation has no benefit. In patients with poor-prognosis GCT or germ cell tumors in relapse, however, strategies for a better and earlier response evaluation in order to modify ineffective but toxic chemotherapy regimens are warranted. Bokemeyer et al. [72] addressed this problem in 23 patients with relapsed germ cell cancer enrolled in a high-dose salvage chemotherapy program. FDG PET scans were recorded before conventional-dose induction and before high-dose treatment together with the usual tumor marker profiles and CT scans. The results were compared with the histologic response and/or the clinical course over 6 months following high-dose treatment (relapse versus freedom from progression). FDG PET showed a sensitivity, specificity, PPV, and NPV of 100, 78, 88 and 100%, respectively, and was superior to tumor marker assays, CT and both of them (Fig. 28.2). It therefore seemed to be a valuable addition to the established prognostic model for high-dose chemotherapy of germ cell tumors [73]. However, the authors cautioned that, at this point in time, it was not justified to derive treatment decisions from PET results alone. Larger studies are necessary to confirm this approach.

Summary

To date FDG PET has not been proven to be a reliable tool for changing treatment decisions in poor-risk or relapsed germ cell tumor patients.

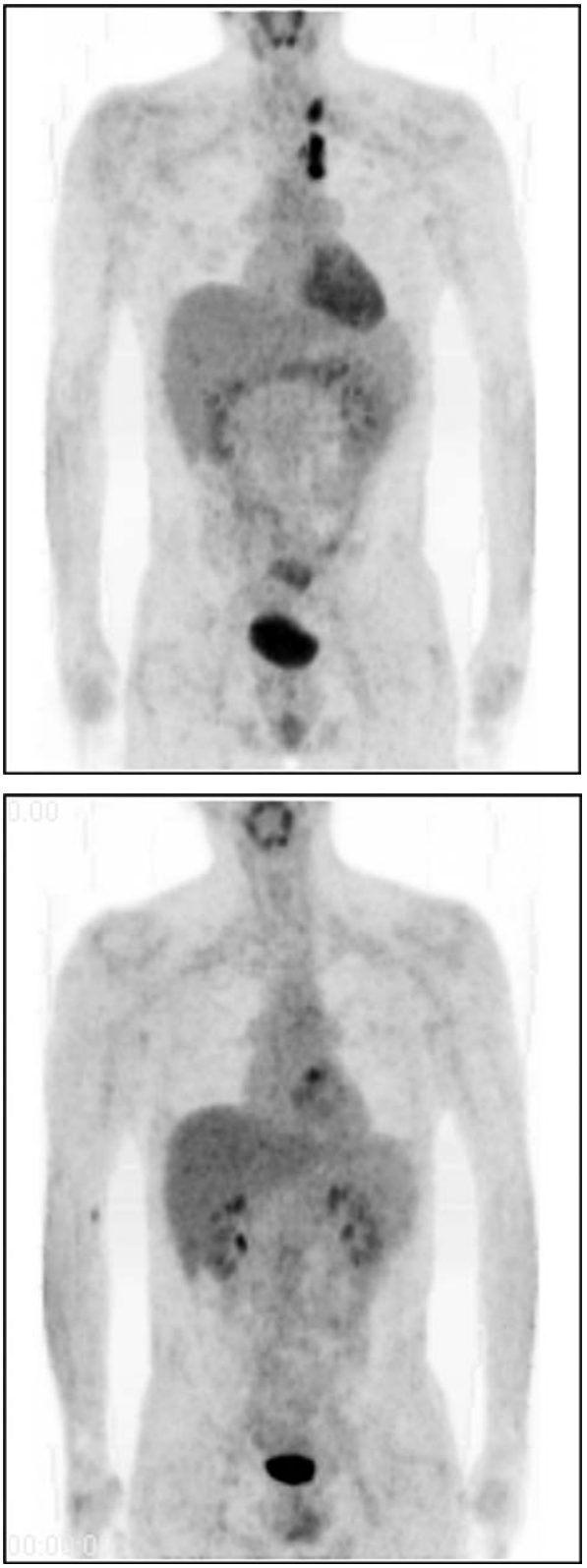

Fig. 28.2 a) Residual mediastinal lymph nodes, SGCT; true positive PET scan after completion of first line chemotherapy with clinical relapse 2 months later. b) True negative FDG PET in the same patient after first cycle of high dose chemotherapy. No residual tumor resection. Clinical follow-up and shrinkage of mediastinal residuals for >3 years

Relapse

Diagnosis of Relapse

About 20% of all patients with germ cell cancer relapse. Diagnostic evidence for this clinical situation is a rise in tumor marker levels and radiologic (rarely clinical) signs. For those who relapse with rising marker levels and unequivocal radiologic/clinical signs of progressive disease the guidelines for management are clear and well established: salvage chemotherapy, standard or high dose, followed by salvage surgery, or primary salvage surgery are the standard treatment options. For all other relapses FDG PET might be a valuable diagnostic tool. The key situations include

1. Rising tumor markers unmatched by clinical/radiologic abnormalities
2. Radiologic evidence of a new lesion or an increase in the volume of a pre-existing one unassociated with rising marker levels
3. Rising tumor marker levels in the presence of multiple residual lesions unchanged in size.

Although FDG PET appears to hold promise for answering these questions, only few reports on relapsing germ cell cancer patients, all of them retrospective or just case reports, are available [60, 62, 74].

Hain et al. [60] reported all 12 positive PET scans of 23 patients in marker-only relapse to be truly positive. PET clearly identified the site of the disease. However, 4 out of 11 scans were false negative. Subsequently, three of these PET scans turned positive and were the only imaging investigation to identify the site of the disease. In a report from France [74] FDG PET also was the only imaging study to identify the site of the disease in five out of seven patients with elevated markers. Sanchez et al. [62] found three true positive and two true negative FDG PET scans in patients with elevated markers and non-contributory CT scans and patients with normal marker levels and increasing lesions on CT, respectively, the latter mature teratoma by histologic evidence.

A patient reported by Reinhardt et al. [75] presented with negative markers and a negative FDG PET scan of a growing retroperitoneal bulk. Not surprisingly, this bulky disease proved to be a mature ”growing teratoma” on histology and therefore was true negative. In another case report FDG PET showed a contralateral testicular lesion in a clinically and sonographically normal testicle to be the underlying cause of an AFP rise [76].

Summary

FDG PET can be expected to be helpful for planning elective salvage surgery in chemoresistant patients and in those with multiple residual lesions to be removed. However, evidence from pertinent studies is not available.

Conclusions

In GCT, FDG PET is not superior to conventional staging tools for staging at presentation. It is not safe for detecting lesions less than 1 cm in size and mature teratoma.

FDG PET should be used as a standard diagnostic tool in patients with pure seminomatous residual lesions. It predicts the persistence of viable tumor in this clinical situation with a high diagnostic accuracy. FDG PET-negative SGCT residual lesions may be observed safely.

NSGCT patients with residual masses do not benefit from FDG PET. Residual mature teratoma, which is PET-negative, will be missed, and has to be resected at any rate, just like PET-positive residual lesions.

In relapsing patients with a mismatch between tumor marker levels and imaging data, FDG PET may be helpful in selected cases, particularly if salvage surgery is considered.

References

1. Carlsson-Farrelly E, Boquist L, Ljungberg B. Accuracy of clinical staging in non-seminomatous testicular cancer – a single centre experience of retroperitoneal lymph node dissection. Scand J Urol Nephrol. 1995;29(4):501–6.
2. Fernandez EB, et al. Retroperitoneal imaging with third and fourth generation computed axial tomography in clinical stage I nonseminomatous germ cell tumors. Urology. 1994;44(4):548–52.
3. Rustin GJ, et al. Consensus statement on circulating tumour markers and staging patients with germ cell tumours. Prog Clin Biol Res. 1990;357:277–84.
4. Kubota R, et al. Intratumoral distribution of fluorine-18-fluorodeoxyglucose in vivo: high accumulation in macrophages and granulation tissues studied by microautoradiography. J Nucl Med. 1992;33(11):1972–80.
5. Wilson CB, et al. Imaging metastatic testicular germ cell tumours with 18FDG positron emission tomography: prospects for detection and management. Eur J Nucl Med. 1995;22(6):508–13.
6. Hoekstra OS, et al. Early treatment response in malignant lymphoma, as determined by planar fluorine-18-fluorodeoxyglucose scintigraphy. J Nucl Med. 1993;34(10):1706–10.
7. Wahl RL, et al. Metabolic monitoring of breast cancer chemohormonotherapy using positron emission tomography: initial evaluation. J Clin Oncol. 1993;11(11):2101–11.
8. Engel H, et al. Whole-body PET: physiological and artifactual fluorodeoxyglucose accumulations. J Nucl Med. 1996;37(3):441–6.
9. Keyes JW Jr. SUV: standard uptake or silly useless value? J Nucl Med. 1995;36(10):1836–9.
10. Landoni C, et al. Comparison of dual-head coincidence PET versus ring PET in tumor patients. J Nucl Med. 1999;40(10):1617–22.
11. Bomanji JB, Costa DC, Ell PJ. Clinical role of positron emission tomography in oncology. Lancet Oncol. 2001;2(3):157–64.
12. Lienhard GE, et al. How cells absorb glucose. Sci Am. 1992;266(1):86–91.
13. Nabi HA, Zubeldia JM. Clinical applications of (18)F-FDG in oncology. J Nucl Med Technol. 2002;30(1):3–9; quiz 10–1.
14. Kole AC, et al. L-[1-carbon-11]tyrosine imaging of metastatic testicular nonseminoma germ-cell tumors. J Nucl Med.1998;39(6):1027–9.
15. Vesselle HJ, Miraldi FD. FDG PET of the retroperitoneum: normal anatomy, variants, pathologic conditions, and strategies to avoid diagnostic pitfalls. Radiographics. 1998;18(4):805–23; discussion 823–4.
16. Cremerius U, et al. FDG PET for detection and therapy control of metastatic germ cell tumor. J Nucl Med. 1998;39(5):815–22.
17. Nuutinen JM, et al. Detection of residual tumours in postchemotherapy testicular cancer by FDG-PET. Eur J Cancer. 1997;33(8):1234–41.
18. Strauss LG. Fluorine-18 deoxyglucose and false-positive results: a major problem in the diagnostics of oncological patients. Eur J Nucl Med. 1996;23(10):1409–15.
19. Engenhart R, et al. Therapy monitoring of presacral recurrences after high-dose irradiation: value of PET, CT, CEA and pain score. Strahlenther Onkol. 1992;168(4):203–12.
20. Haberkorn U, et al. PET studies of fluorodeoxyglucose metabolism in patients with recurrent colorectal tumors receiving radiotherapy. J Nucl Med. 1991;32(8):1485–90.
21. Cohade C, Wahl RL. PET scanning and measuring the impact of treatment. Cancer J. 2002;8(2):119–34.
22. Hain SF, et al. Fluorodeoxyglucose PET in the initial staging of germ cell tumours. Eur J Nucl Med. 2000;27(5):590–4.
23. Stroobants S, et al. 18FDG-Positron emission tomography for the early prediction of response in advanced soft tissue sarcoma treated with imatinib mesylate (Glivec). Eur J Cancer. 2003;39(14):2012–20.
24. Albers P, et al. Positron emission tomography in the clinical staging of patients with stage I and II testicular germ cell tumors. Urology. 1999;53(4):808–11.
25. Cremerius U, et al. Does positron emission tomography using 18-fluoro-2-deoxyglucose improve clinical staging of testicular cancer? – Results of a study in 50 patients. Urology. 1999;54(5):900–4.
26. Hofer C, et al. Diagnosis and monitoring of urological tumors using positron emission tomography. Eur Urol. 2001;40(5):481–7.
27. Muller-Mattheis V, et al. Positron emission tomography with [18 F]-2-fluoro-2-deoxy-D-glucose (18FDG-PET) in diagnosis of retroperitoneal lymph node metastases of testicular tumors. Urologe A. 1998;37(6):609–20.
28. Spermon JR, et al. The role of (18)fluoro-2-deoxyglucose positron emission tomography in initial staging and re-staging after chemotherapy for testicular germ cell tumours. BJU Int. 2002;89(6):549–56.
29. Tsatalpas P, et al. Diagnostic value of 18F-FDG positron emission tomography for detection and treatment control of malignant germ cell tumors. Urol Int. 2002;68(3):157–63.
30. De Wit M, Hartmann M, Brenner W, Weißbach L, Amthauer H, Franzius C, et al. [18F]-FDG-PET in germ cell tumors following chemotherapy: Results of the German multicenter trial. J Clin Oncol, 2006 ASCO Annual Meeting Proceedings Part I. 24(18S) (June 20 Suppl) 2006:4521.
31. Eary JF. Nuclear medicine in cancer diagnosis. Lancet. 1999;354(9181):853–7.

32. Hustinx R, et al. Clinical evaluation of whole-body 18F-fluorodeoxyglucose positron emission tomography in the detection of liver metastases. Ann Oncol. 1998;9(4):397–401.
33. Lowe VJ, et al. Prospective investigation of positron emission tomography in lung nodules. J Clin Oncol. 1998;16(3): 1075–84.
34. Moog F, et al. 18-F-fluorodeoxyglucose-positron emission tomography as a new approach to detect lymphomatous bone marrow. J Clin Oncol. 1998;16(2):603–9.
35. Regelink G, et al. Detection of unknown primary tumours and distant metastases in patients with cervical metastases: value of FDG-PET versus conventional modalities. Eur J Nucl Med Mol Imaging. 2002;29(8):1024–30.
36. Spaepen K, et al. Early restaging positron emission tomography with (18)F-fluorodeoxyglucose predicts outcome in patients with aggressive non-Hodgkin's lymphoma. Ann Oncol. 2002;13(9): 1356–63.
37. Jerusalem G, et al. Early detection of relapse by whole-body positron emission tomography in the follow-up of patients with Hodgkin's disease. Ann Oncol. 2003;14(1):123–30.
38. Jerusalem G, et al. Whole-body positron emission tomography using 18F-fluorodeoxyglucose for posttreatment evaluation in Hodgkin's disease and non-Hodgkin's lymphoma has higher diagnostic and prognostic value than classical computed tomography scan imaging. Blood. 1999;94(2):429–33.
39. Kostakoglu L, et al. PET predicts prognosis after 1 cycle of chemotherapy in aggressive lymphoma and Hodgkin's disease. J Nucl Med. 2002;43(8):1018–27.
40. Schoder H, et al. Intensity of 18fluorodeoxyglucose uptake in positron emission tomography distinguishes between indolent and aggressive non-Hodgkin's lymphoma. J Clin Oncol. 2005;23(21): 4643–51.
41. Juweid ME, et al. Response assessment of aggressive non-Hodgkin's lymphoma by integrated International Workshop Criteria and fluorine-18-fluorodeoxyglucose positron emission tomography. J Clin Oncol. 2005;23(21):4652–61.
42. Stephens AW, et al. Positron emission tomography evaluation of residual radiographic abnormalities in postchemotherapy germ cell tumor patients. J Clin Oncol. 1996;14(5):1637–41.
43. Donohue JP, et al. The role of retroperitoneal lymphadenectomy in clinical stage B testis cancer: the Indiana University experience (1965 to 1989). J Urol. 1995;153(1):85–9.
44. Stephenson AJ, et al. Retroperitoneal lymph node dissection for nonseminomatous germ cell testicular cancer: impact of patient selection factors on outcome. J Clin Oncol. 2005;23(12): 2781–8.
45. Gatti JM, Stephenson RA. Staging of testis cancer. Combining serum markers, histologic parameters, and radiographic imaging. Urol Clin North Am. 1998;25(3):397–403.
46. Hilton S, et al. CT detection of retroperitoneal lymph node metastases in patients with clinical stage I testicular nonseminomatous germ cell cancer: assessment of size and distribution criteria. AJR Am J Roentgenol. 1997;169(2):521–5.
47. Donohue JP, et al. Retroperitoneal lymphadenectomy for clinical stage A testis cancer (1965 to 1989): modifications of technique and impact on ejaculation. J Urol. 1993;149(2):237–43.
48. Pont J, et al. Adjuvant chemotherapy for high-risk clinical stage I nonseminomatous testicular germ cell cancer: long-term results of a prospective trial. J Clin Oncol. 1996;14(2):441–8.
49. Lassen U, et al. Positron emission tomography with 18F-Fluoro-Deoxyglucose in clinical stage I non-seminomatous germ cell tumors. ASCO Annual Meeting. 2000:1337.
50. Lassen U, et al. Whole-body FDG-PET in patients with stage I non-seminomatous germ cell tumours. Eur J Nucl Med Mol Imaging. 2003;30(3):396–402.
51. Huddart RA, O'Doherty MJ, Padhani A, Rustin GJS, Mead GM, Joffe JK, et al. 18Fluorodeoxyglucose positron emission tomography in the prediction of relapse in patients with high-risk, clinical stage I nonseminomatous germ cell tumors: Preliminary Report of MRC Trial TE22—The NCRI Testis Tumour Clinical Study Group. J Clin Onocol. 2007;3090–5.
52. Warde P, et al. Prognostic factors for relapse in stage I seminoma managed by surveillance: a pooled analysis. J Clin Oncol. 2002;20(22):4448–52.
53. Oliver RT, Mason MD, Mead GM, von der Maase H, Rustin GJ, Joffe JK, et al. MRC TE19 collaborators and the EORTC 30982 collaborators. Radiotherapy versus single-dose carboplatin in adjuvant treatment of stage I seminoma: a randomised trial. Lancet. 2005;366(9482):293–300.
54. Oliver RT, Mead GM, Fogarty PJ, et al. Radiotherapy versus carboplatin for stage I seminoma: Updated analysis of the MRC/EORTC randomized trial (ISRCTN27163214). J Clin Oncol 2008;26 (May 20 suppl; abstr 1).
55. Donohue JP, et al. Correlation of computerized tomographic changes and histological findings in 80 patients having radical retroperitoneal lymph node dissection after chemotherapy for testis cancer. J Urol. 1987;137(6):1176–9.
56. Toner GC, et al. Adjunctive surgery after chemotherapy for nonseminomatous germ cell tumors: recommendations for patient selection. J Clin Oncol. 1990;8(10):1683–94.
57. Fizazi K, et al. Viable malignant cells after primary chemotherapy for disseminated nonseminomatous germ cell tumors: prognostic factors and role of postsurgery chemotherapy – results from an international study group. J Clin Oncol. 2001;19(10): 2647–57.
58. Loehrer PJ Sr, et al. Teratoma following cisplatin-based combination chemotherapy for nonseminomatous germ cell tumors: a clinicopathological correlation. J Urol. 1986;135(6):1183–9.
59. Steyerberg EW, et al. Validity of predictions of residual retroperitoneal mass histology in nonseminomatous testicular cancer. J Clin Oncol. 1998;16(1):269–74.
60. Hain SF, et al. Fluorodeoxyglucose positron emission tomography in the evaluation of germ cell tumours at relapse. Br J Cancer. 2000;83(7):863–9.
61. Kollmannsberger C, et al. Prospective comparison of [18F] fluorodeoxyglucose positron emission tomography with conventional assessment by computed tomography scans and serum tumor markers for the evaluation of residual masses in patients with nonseminomatous germ cell carcinoma. Cancer. 2002;94(9):2353–62.
62. Sanchez D, et al. 18F-fluoro-2-deoxyglucose-positron emission tomography in the evaluation of nonseminomatous germ cell tumours at relapse. BJU Int. 2002;89(9):912–6.
63. Sugawara Y, et al. Germ cell tumor: differentiation of viable tumor, mature teratoma, and necrotic tissue with FDG PET and kinetic modeling. Radiology. 1999;211(1):249–56.
64. De Santis M, et al. Predictive impact of 2-18fluoro-2-deoxy-D-glucose positron emission tomography for residual postchemotherapy masses in patients with bulky seminoma. J Clin Oncol. 2001;19(17):3740–4.
65. Puc HS, et al. Management of residual mass in advanced seminoma: results and recommendations from the Memorial Sloan-Kettering Cancer Center. J Clin Oncol. 1996;14(2):454–60.
66. Schultz SM, et al. Management of postchemotherapy residual mass in patients with advanced seminoma: Indiana University experience. J Clin Oncol. 1989;7(10):1497–503.
67. Ganjoo KN, et al. Positron emission tomography scans in the evaluation of postchemotherapy residual masses in patients with seminoma. J Clin Oncol. 1999;17(11):3457–60.
68. De Santis M, et al. 2-18fluoro-deoxy-D-glucose positron emission tomography is a reliable predictor for viable tumor

in postchemotherapy seminoma: an update of the prospective multicentric SEMPET trial. J Clin Oncol. 2004;22(6): 1034–9.
69. Findlay M, et al. Noninvasive monitoring of tumor metabolism using fluorodeoxyglucose and positron emission tomography in colorectal cancer liver metastases: correlation with tumor response to fluorouracil. J Clin Oncol. 1996;14(3):700–8.
70. Schelling M, et al. Positron emission tomography using [(18)F]Fluorodeoxyglucose for monitoring primary chemotherapy in breast cancer. J Clin Oncol. 2000;18(8): 1689–95.
71. Smith IC, et al. Positron emission tomography using [(18)F]-fluorodeoxy-D-glucose to predict the pathologic response of breast cancer to primary chemotherapy. J Clin Oncol. 2000;18(8): 1676–88.
72. Bokemeyer C, et al. Early prediction of treatment response to high-dose salvage chemotherapy in patients with relapsed germ cell cancer using [(18)F]FDG PET. Br J Cancer. 2002;86(4): 506–11.
73. Beyer J, et al. High-dose chemotherapy as salvage treatment in germ cell tumors: a multivariate analysis of prognostic variables. J Clin Oncol. 1996;14(10):2638–45.
74. Maszelin P, et al. Fluorodeoxyglucose (FDO) positron emission tomography (PET) in testicular germ cell tumors in adults: preliminary French clinical evaluation, development of the technique and its clinical applications. Prog Urol. 2000;10(6):1190–9.
75. Reinhardt MJ, et al. FDG-PET evaluation of retroperitoneal metastases of testicular cancer before and after chemotherapy. J Nucl Med. 1997;38(1):99–101.
76. Wolf G, et al. Diagnosis of a contralateral second testicular carcinoma by F18-FDG PET. Onkologie. 2003;26(2):155–7.

Chapter 34

Considerations: Imaging in Penis Carcinoma

S. Horenblas, B.K. Kroon, R.A. Valdés Olmos, and C.A. Hoefnagel

Introduction

Malignant tumors of the penis consist of 95% of the cases of squamous cell carcinoma. The other 5% comprises of other tumors originating in the skin, like melanoma and basal cell cancer, or tumors arising from elements of cavernous tissue like soft tissue tumors [1–3]. Ideally, imaging modalities should help the clinician in deciding on the appropriate therapy of the primary tumor by exactly delineating the extent of the tumor and invasion in various structures of the penis, like the cavernous tissues and the urethra. Squamous cell carcinoma shows a very strong tendency for lymphatic spread first, with hematogenic spread in very advanced cases only [4]. Timely management of lymph node metastasis is of utmost importance [5, 6]. Imaging should also inform the clinician on the absence or presence of regional metastases in the groin area. In more advanced cases knowledge of spread to second echelon lymph nodes in the pelvic region and further spread to retroperitoneal lymph nodes is essential for a rational approach.

Table 34.1 1987 TNM Classification [8]

T-Primary tumor
T X Primary tumor cannot be assessed
TO No evidence of primary tumor
Tis Carcinoma in situ
Ta Non-invasive verrucous carcinoma
TI Tumor invades subepithelial connective tissue
T2 Tumor invades corpus spongiosum or cavernosum
T3 Tumor invades urethra or prostate
T4 Tumor invades other adjacent structures
N-Regional lymph nodes
NX Regional lymph nodes cannot be assessed
NO No regional lymph node metastasis
NI Metastasis in a single superficial inguinal lymph node
N2 Metastasis in multiple or bilateral superficial inguinal lymph nodes
N3 Metastasis in deep inguinal or pelvic Iymph node(s), unilateral or bilateral
M-Distant metastasis
MX Distant metastasis cannot be assessed
MO No distant metastasis
MI Distant metastasis
Stage grouping
Stage O Tis NO MO Ta NO MO
Stage I TI NO MO
Stage II TI NI MO T2 NO, NI MO
Stage III TI N2 MO T2 N2 MO T3 NO, NI, N2 MO
Stage IV T4 Any N MO Any T N3 MO Any T Any N MI

Imaging of the Primary Tumor

The extent of the primary tumor in squamous cell carcinoma of the penis has important prognostic and therapeutic implications. The prognostic difference between deeply infiltrating tumors and superficially growing tumors has been recognized for a long time and is expressed already in the first TNM classification system for squamous cell carcinoma of the penis [7]. Size of the tumor was surpassed by depth of infiltration as a classification criterion in the most recent classification [8]. A distinction was made between tumors infiltrating into the deeper structures of the penis and tumors invading the superficial layers only (Table 34.1) This distinction, how important this may be, is not easily made on clinical grounds only.

The main issue in the management of the primary tumor is the decision whether to amputate or not. Standard partial penile amputation as a treatment for localized squamous cell carcinoma is increasingly being replaced by methods that conserve the penis [9, 10]. Main danger is the risk for local recurrence, which increases proportionally with size and depth of infiltration of the tumor. Therefore, the extension of the primary carcinoma must be assessed with great care. Staging on clinical grounds only is not always easy, as the often accompanying infection can give the impression of deep infiltration while microscopic invasion can easily be missed. Comparing clinical and pathological staging in a series with almost 100 patients with squamous cell cancer

S. Horenblas (✉)
Netherlands Cancer Institute/Antoni van Leeuwenhoek Hospital, Plesmanlaan 121, 1066 CX, Amsterdam, s.horenblas@nki.nl

J.J.M.C.H. de la Rosette et al. (eds.), *Imaging in Oncological Urology*,
DOI 10.1007/978-1-84628-759-6_34,

showed the following differences: in 10% of the cases the clinical stage was higher compared to the pathological stage ("overstaging"), in 16% of the tumors the pathological stage was higher than the clinical one ("understaging"). Overall a 26% difference between clinical and pathological stage was found, almost similar to a 23% difference in a study from Maiche et al. [11, 12]. Reasons for these discrepancies were clinically undetected infiltration in the subepithelial tissue or corpus spongiosum, infection, and edema masking the real size of the tumor and giving a false impression of infiltration.

Can imaging contribute to more accurate staging? Various imaging techniques have been evaluated for this purpose [13–18].

Cross-Sectional Imaging Techniques

Ultrasound

Various distinctive structures of the penis can be depicted on ultrasound investigation and used for staging penile carcinoma. The tumor itself is mostly shown as a hypoechoic lesion (Fig. 34.1). It can be distinguished from the urethra. Introducing a urethral catheter can aid in delineating the tumor. The tunica albuginea surrounding both corpora cavernosa is seen as a hyperechoic structure (Fig. 34.2). Ultrasound was shown to reliably give the extent of infiltration into the corpora cavernosa, but was not reliable enough in discerning the true extent of infiltration into the corpus spongiosum of the glans [19].

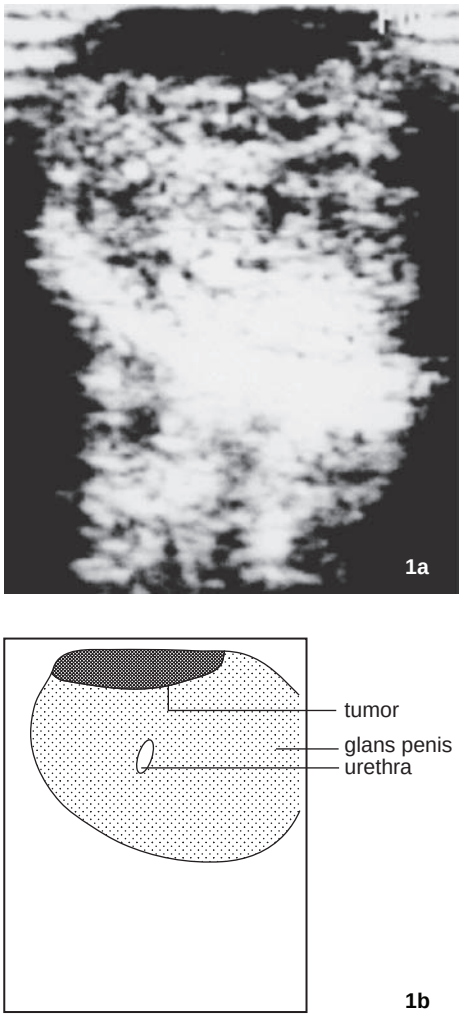

Fig. 34.1 Ultrasound examination of penile carcinoma (a) with schematic representation of distinct structures (b), showing a hypoechoic lesion

CT Scanning

Computerized tomography is limited by its ability to image in one plane only and the poor soft tissue contrast. While it has been used extensively for the detection of nodal metastases, it has been used rarely for imaging the primary tumor, as the tumor and surrounding corporal bodies are poorly differentiated [18, 20, 21]. One can conclude that CT scanning does not play a role in the imaging of the primary tumor.

Magnetic Resonance Imaging (MRI)

In contrast to CT scan, MRI imaging is not limited by imaging in one plane. Moreover, soft tissue contrast is much better than with CT scan. Lont et al. analyzed the accuracy of MRI staging of the primary tumor [17]. MR images were obtained in the axial plane using T1-weighted spin echo (T1-SE) and T2-weighted turbo-spin echo (T2-TSE) sequences. Sagittal images were acquired using a short inversion recovery sequence and T1-SE sequences, before and after administering an intravenous contrast agent (gadolinium based). Tumor identification was mainly based on the presence of lesions with low signal intensity relative to the corporal bodies on the T1- or the T2-weighted images (Figs. 34.3 and 34.4). It was concluded that because of the possibility of imaging in various planes and because of the ability to visualize other structures of the penis, MRI can be useful in doubt of the true proximal extent of the tumor.

In order to improve imaging of the primary tumor, MRI was combined with artificial erection and compared with pathologic staging in nine cases of penile cancer. T1-weighted and T2-weighted MRI with and without contrast was obtained using a phased array coil. The MRI and pathologic staging coincided in eight of nine patients. In one patient no tumor was detected at MRI. Despite the differences between clinical staging and MRI staging, this had no therapeutical consequences [22].

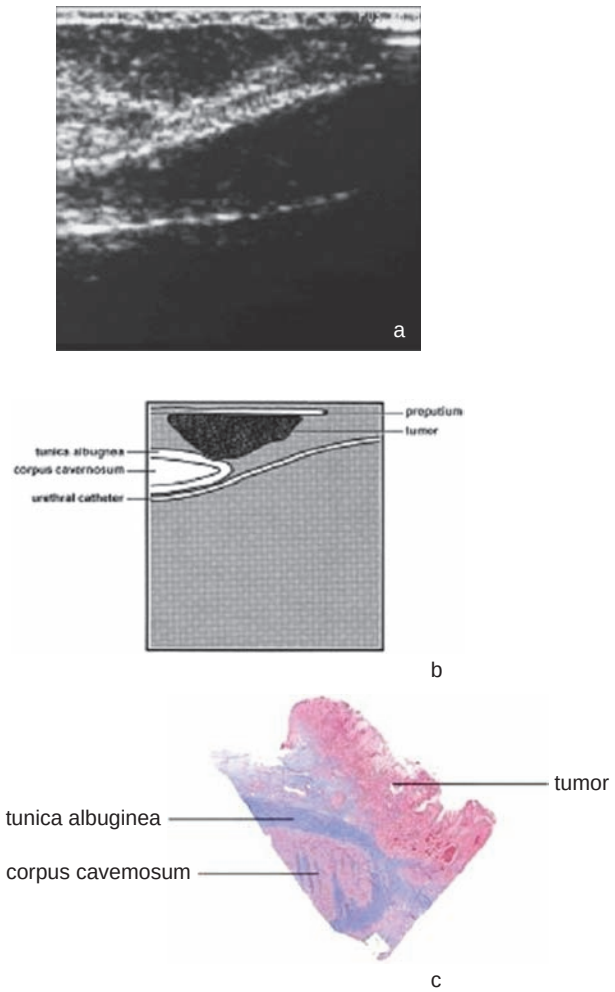

Fig. 34.2 Ultrasound examination of penile carcinoma (a) with schematic representation of distinct structures (b), showing the tumor abutting the tunica albuginea, without invading it. Histology (c) confirms the ultrasound observation (tumor not invading the tunica albuginea)

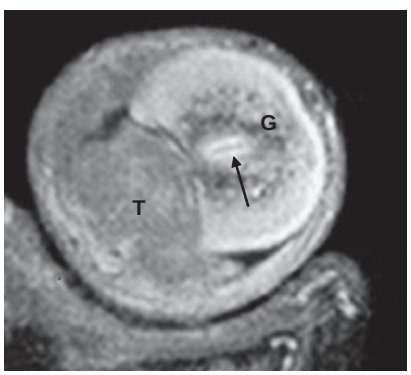

Fig. 34.3 MRI (T1 SPIR) with contrast in the transversal plane at a distal level of the penis in a patient with a T2 tumor. The tumor is seen as a low signal mass, clearly distinguished from the glans penis (T = tumor, G = glans penis, arrow indicates urethra)

Accuracy of Physical Examination, Ultrasound, and MRI

The accuracy of physical examination, ultrasound investigation, and magnetic resonance imaging (MRI) was compared in 33 patients [17]. All patients underwent a radiological evaluation with ultrasonography and MRI, the former using an SDD 280 LS scanner (Aloka Corp., Tokyo, Japan) with a 7.5 MHz linear-array small-parts transducer, and the latter using a 1.5 T Magnetom scanner (Siemens GmbH, Germany) with a small surface coil. An ultrasonography gel pad was used to avoid artifacts, and a urethral catheter was introduced for identification. The tumor was identified by the presence of hypoechoic lesions on the ultrasonograms that were not consistent with normal penile anatomy. Tumor size was determined in two directions using standard calipers on the ultrasonogram and in three planes on MRI. Invasion by tumor of the subepithelial stroma, corpus spongiosum, corpora cavernosa, and urethra was assessed. Infiltration depth was measured. After comparing the findings of the various investigations with histopathology, physical examination was more reliable for assessing tumor size than were ultrasonography and MRI. Furthermore physical examination predicted corpus cavernosum infiltration with the highest positive predictive value and was accurate for determining the presence of deep infiltration, missing substantial infiltration in only 2 of 33 patients (Table 34.2). For infiltration into the corpus spongiosum of the glans, the following values for positive predictive value and sensitivity were found: 94, 92, and 91% and 68, 92, and 80%, respectively, for physical examination, ultrasonography, and MRI. There were no false-positive findings of infiltration. MRI was the most sensitive method for determining cavernosal infiltration but at the cost of some false-positive results.

Imaging of Lymph Nodes

Squamous cell carcinoma of the penis metastasizes first to the inguinal lymph nodes and from there to the pelvic nodes. Metastases to the pelvic nodes without inguinal involvement (skip metastases) have hardly been observed, except an occasional case. By definition clinically occult metastasis are not detected by physical examination. These clinically node-negative patients present a challenge for additional imaging as approximately 20% will harbor clinically undetectable metastases. Non-invasive methods to detect these metastases are unreliable, but there is a clinical need to find occult metastases at the earliest possible stage, because survival is related to presence and extent of nodal involvement [5, 6, 23]. The optimum management of patients with clinically node-negative groins is controversial. A surveillance

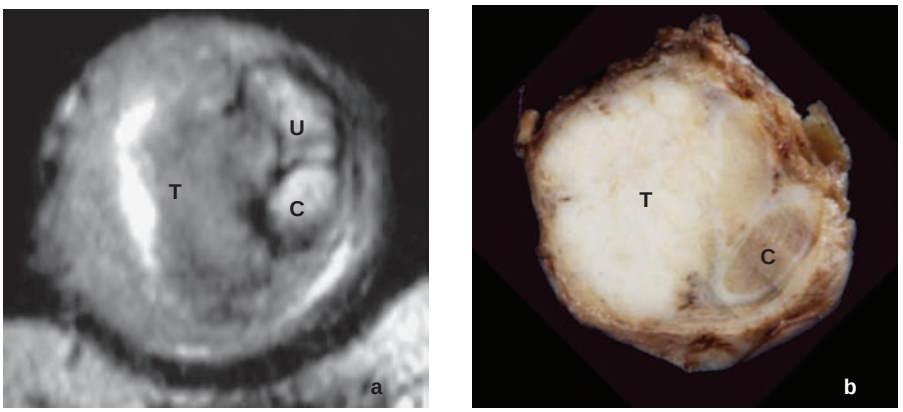

Fig. 34.4 (a) MRI (T1 TSE) without contrast in the transversal plane at a more proximal level of the penis in another patient with a T2 tumor. The tumor is seen as a mass with increased signal involving the corpus cavernosum. Some fluid collection between the preputium and the tumor is visible (T = tumor, C = corpus cavernosum, U = urethra). (b) Cross-section of the corresponding macroscopic specimen illustrates the findings on MRI, with macroscopic involvement of the corpus cavernosum (T = tumor, C = corpus cavernosum). The urethra was dissected during surgery

Table 34.2 The positive predictive value, sensitivity, and specificity of infiltration of the corpus cavernosum, as determined by physical examination, ultrasound, and MRI

Cavernosum infiltration	Positive predictive value	Sensitivity	Specificity
Physical examination	100%	71%	100%
Ultrasound	67%	57%	97%
MRI	75%	100%	91%

policy risks the patients presenting with metastasis at a stage where cure is no longer possible. On the other hand, early inguinal lymphadenectomy in all clinically node-negative patients is unnecessary in up to 80% and associated with substantial morbidity [24]. Thus better staging procedures are mandatory to improve the detection of occult metastasis and to decrease the number of unnecessary lymph node dissections. Detection of lymph node metastases in the groin and pelvis on CT scan or MRI is detected mainly by change of size. Lymph nodes smaller than 1 cm are usually considered normal. A distortion of the internal architecture by a small metastatic deposit without change of size was only visible by lymphangiography until recently [11]. Promising techniques, like modern ultrasound and MRI, using ultrasmall particles of iron oxide (USPIO), are underway to detect these occult metastases more reliably.

Patients presenting with inguinal lymph node enlargement are easily detected by physical examination. However, on average only half of them harbor lymph node metastasis, the other half is due to benign enlargement because of the often concomitant inflammation [25]. A distinction between absence and presence of lymph node metastases can be made on the basis of fine-needle aspiration biopsy guided by ultrasound or CT scanning. Understandably only a tumor-positive outcome is reliable. In patients with proven inguinal lymph node metastasis, imaging with CT scan or MRI is useful for the determination of the extent of metastatic spread.

Cross-Sectional Imaging Techniques

Ultrasound

Thanks to the high-resolution probes, ultrasound scanning is increasingly reliable in detecting occult metastases. Modern ultrasound not only visualizes alteration in size, shape, and contour of lymph nodes but also depicts changes in the cortical and hilar morphology and texture that can reflect the presence of underlying metastasis [26]. Changes in the architecture of the node occur before the node enlarges and these are identified by the radiologist. Currently the spatial resolution limit is around 2 mm. Due to overlap of sonographic features of benign and suspicious lymph nodes, fine-needle aspiration cytology (FNAC) of sonographically suspicious nodes provides a more definitive diagnosis than ultrasound alone. Potential applications have been demonstrated in a number of malignancies [27–30]. In 2001, ultrasound-guided FNAC was introduced as standard staging procedure at the Netherlands Cancer Institute-Antoni van Leeuwenhoek Hospital to improve staging of clinically node-negative penile SCC patients (Figs. 34.5 and 34.6).

The sensitivity of ultrasound-guided FNAC to reveal clinically occult lymph node metastases was 39%, with a 100% specificity. In contrast to penile cancer, ultrasound-guided FNAC has been used extensively in assessing lymph nodes in other malignancies such as breast cancer and melanoma. Sensitivity and specificity rates are about the same as reported for these tumors. With a sensitivity of 39% there is a false-negative rate of 61%, necessitating other means to

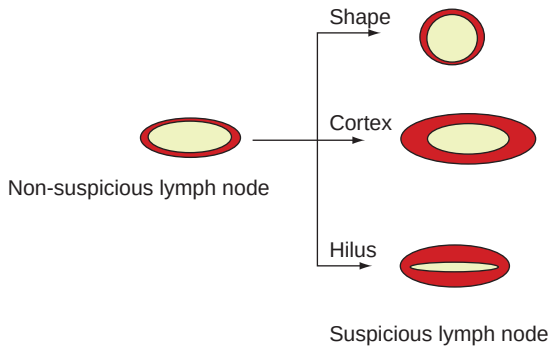

Fig. 34.5 Sonomorphologic lymph node features according to Vassallo et al. lymph node shape, cortex (normal or wide), and hilus (normal, narrow, or absent). Suspicious features for nodal involvement are a round shape, a wide cortex, and a narrow to absent hilus

assess the regional lymph nodes. At our institute we favor a so-called dynamic sentinel node biopsy (DNSB). So far ultrasound-guided FNAC cannot replace DSNB. However, it is a useful tool for preoperative screening of the clinically node-negative groins in patients with penile cancer scheduled to undergo DSNB. The commonest cause of a false-negative DSNB procedure is gross involvement of the sentinel node by tumor cells which prohibits tracer uptake with a false-negative procedure as a result [31]. These nodes in particular might be detected by ultrasound-guided FNAC. Moreover, nodal recurrences, which can occur after a false-negative DSNB procedure, might be detected earlier when compared to physical examination.

What are the causes of false-negative ultrasound results? First, the lymph node may appear abnormal and indeed contain metastatic disease, but the aspirate may fail to extract abnormal cells. This relates to erroneous sampling and can be difficult to overcome in a node with a small metastasis where placement of the needle is crucial. Second, microscopic small foci of metastases might be beyond the resolution of the transducer and therefore not show up on the images [28]. In order to improve the efficiency of ultrasound scanning, the future effort should focus on the reduction of false-negative results. To this end, at least two strategies might be useful. First, the introduction of echogenic contrast has been advocated to increase ultrasound diagnostic power by allowing the identification of indirect features of lymph node metastases. Second, increasing the ultrasound probe ultrafrequency might ameliorate the resolution power, thus allowing the detection of lesions smaller than 2 mm [30]. In addition, a learning phase of the radiologist performing ultrasound-guided FNAC cannot be denied.

CT Scanning

Only one study exists in which the value of CT scanning in detecting regional lymph node metastases is assessed. Regional lymph node invasion that escaped clinical examination was not detected by CT [11]. Positive findings were found only in patients with clinically suspected nodes. Clinical decisions with respect to the management of regional lymph nodes should therefore not be based on negative CT findings. In patients with proved metastasis additional imaging may be of some help in the detection of pelvic node invasion and the determination of the extent of involvement (Fig. 34.7).

MR Imaging

Like in CT scanning, clinically occult metastases will not be detected by conventional MR imaging. MR imaging may be of some help in the detection of pelvic node invasion and the determination of the extent of involvement in patients with proved metastasis.

Recently, however, a promising technique has emerged with the potential to identity occult lymph node metastasis: MRI and ultrasmall particles of iron oxide (USPIO). This novel technique makes use of a lymph node-specific contrast

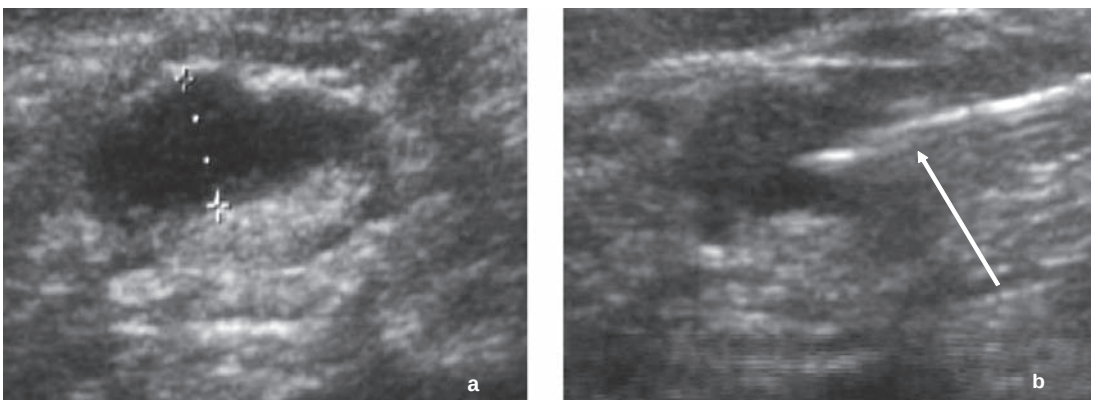

Fig. 34.6 (a) Ultrasound image of suspicious node with a wide cortex. (b) Ultrasound image of FNAC of the same node (arrow indicates needle)

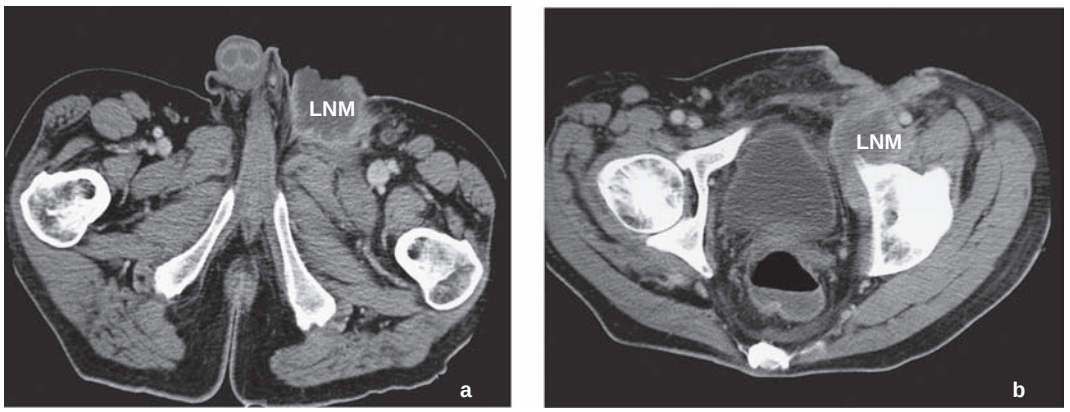

Fig. 34.7 (a) CT image in the transversal plane in a patient with a massive lymph node metastases in the left groin (LNM = lymph node metastasis). (b) Same patient at a more caudal level (LNM = lymph node metastasis)

agent that allows the identification of clinically occult metastasis. This contrast agent, known as ultrasmall particles of iron oxide (USPIO), is injected intravenously and is taken up primarily by macrophages in the lymph nodes. Presence of USPIO in the node results in signal intensity loss (darkening) on T2-weighed sequences. Metastatic growth will displace the macrophages filled with USPIO, and the metastatic part of the node therefore is high in signal intensity (whitening). Thus, metastasis within the lymph node will show as white filling defect. Metastases as small as 1 mm have been detected by using this technique [32]. In a mouse model even as few as 1,000 tumor cells could be depicted [33]. A pilot study in penile carcinoma showed a 100% sensitivity, 97% specificity, and 100% negative predictive value. Improvement of this technique could possibly replace dynamic sentinel node biopsy in the future [34].

Considerations

Primary Tumor

Small superficial tumors can be accurately staged by physical examination only. Imaging can be of help in patients in whom the extent of infiltration into the corpora cannot be determined properly by a physical examination, usually only in patients with locally extensive disease. Because of the high sensitivity for cavernosal infiltration and its precision in determining infiltration depth, MRI is the imaging method of choice. Images in the sagittal plane are particularly useful for detecting the proximal extent of the tumor. In conclusion no imaging modality is more reliable than physical examination for the assessment of the true extent of the tumor. Imaging has no important role in routine clinical management, except where doubt exists about the proximal extent of the primary tumor.

Lymph Node Metastases

Penile carcinoma primarily metastasizes to the inguinal lymph nodes. Even in case of lymphatic metastasis many patients can still be cured. Patients presenting with inguinal lymph node enlargement are easily detected by physical examination. The diagnosis can be proven by fine-needle aspiration cytology, if possible under ultrasonographic guidance. In these patients additional CT or MRI imaging may be of some help in the detection of pelvic node invasion and the determination of the extent of involvement.

Most penile carcinoma patients, however, have no suspicious lymph nodes in their groins. This observation does not exclude the presence of disease. Approximately 25% of the patients harbor occult metastases in these lymph nodes. An important issue in the management of penile carcinoma patients is how to identify these metastases. Elective lymph node dissection is an option but will lead to overtreatment in about 75% of the patients. Moreover, inguinal lymphadenectomy is associated with major morbidity. On the other hand, a wait-and-see policy may have a negative impact on survival. Dynamic sentinel node biopsy is a minimally invasive procedure that enables detection of occult metastasis in clinically node-negative groins. To localize the sentinel node preoperatively, lymphoscintigraphy is performed after peritumoral injections of ^{99m}Tc-labeled nanocolloid tracers. Intraoperatively, the sentinel node can be identified with the aid of a blue dye and a hand-held gamma-ray detection probe. The sensitivity of dynamic sentinel node biopsy in our hands is 84%. Although minimally invasive dynamic sentinel node biopsy is burdened by an 8% complication rate. Moreover,

it requires a patient to be hospitalized. Obviously, the implementation of non-invasive staging methods, i.e., imaging modalities, might improve the quality of life of penile carcinoma patients. The main problem of imaging modalities to detect occult metastases, however, is a low sensitivity. Computerized tomography and magnetic resonance imaging have a very low sensitivity and specificity in the detection of occult lymph node metastases in the groin. Ultrasound with fine-needle aspiration cytology is more accurate. However, as a staging tool, it is inadequate with a sensitivity and specificity of 39 and 100%, respectively, as reported in this chapter. The main problem is the detection of small metastases, i.e., smaller than approximately 3 mm. Positron emission tomography with ^{18}F-fluorodeoxyglucose (FDG-PET) has been advocated to detect occult lymph node metastases in several types of cancer. This technique relies not solely on anatomic identification but largely on physiological characterization of cells. However, the visualization by FDG-PET requires a minimum diameter of about 3 mm, and this technique is therefore not a good alternative for dynamic sentinel node biopsy in staging patients with clinically node-negative penile carcinoma. Magnetic resonance lymphangiography is a promising technique in the detection of occult lymph node metastases. Metastases as small as 1 mm have been detected by using this technique. Preliminary results of this technique in penile carcinoma are promising. Improvement of this technique could possibly replace dynamic sentinel node biopsy in the future.

References

1. Liegl B, Regauer S. Penile clear cell carcinoma. a report of 5 cases of a distinct entity. Am J Surg Pathol. 2004;28:1513.
2. Sanchez-Ortiz R, Huang SF, Tamboli P, et al. Melanoma of the penis, scrotum and male urethra. a 40-year single institution experience. J Urol. 2005;173:1958.
3. Stancik I, Holtl W. Penile cancer. review of the recent literature. Curr Opin Urol. 2003;13:467.
4. Horenblas S, van Tinteren H, Delemarre JF, et al. Squamous cell carcinoma of the penis. III. Treatment of regional lymph nodes. J Urol. 1993;149:492.
5. Ornellas AA, Seixas AL, Marota A, et al. Surgical treatment of invasive squamous cell carcinoma of the penis. retrospective analysis of 350 cases. J Urol. 1994;151:1244.
6. Kroon BK, Horenblas S, Lont AP, et al. Patients with penile carcinoma benefit from immediate resection of clinically occult lymph node metastases. J Urol. 2005;173:816.
7. Harmer MH. TNM classification of malignant tumors. UICC. 3rd ed. Geneva; 1978.
8. International Union Against Cancer. Penis. In: Hermanek P, Sobin LH, editors. TNM classification of malignant tumours. 4th ed. Berlin Heidelberg: Springer Verlag; 1987.
9. Mohs FE, Snow SN, Messing EM, et al. Microscopically controlled surgery in the treatment of carcinoma of the penis. J Urol. 1985;133:961.
10. Windahl T, Hellsten S. Laser treatment of localized squamous cell carcinoma of the penis. J Urol. 1995;154:1020.
11. Horenblas S, van Tinteren H, Delemarre JF, et al. Squamous cell carcinoma of the penis: accuracy of tumor, nodes and metastasis classification system, and role of lymphangiography, computerized tomography scan and fine needle aspiration cytology. J Urol. 1991;146:1279.
12. Maiche AG, Pyrhonen S. Clinical staging of cancer of the penis. By size? By localization? or By depth of infiltration? Eur Urol. 1990;18:16.
13. de Kerviler E, Ollier P, Desgrandchamps F, et al. Magnetic resonance imaging in patients with penile carcinoma. Br J Radiol. 1990;68:704.
14. Hricak H, Marotti M, Gilbert TJ, et al. Normal penile anatomy and abnormal penile conditions. evaluation with MR imaging. Radiology. 1988;169:683.
15. Kageyama S, Ueda T, Kushima R, et al. Primary adenosquamous cell carcinoma of the male distal urethra. magnetic resonance imaging using a circular surface coil. J Urol. 1997;158:1913.
16. Kawada T, Hashimoto K, Tokunaga T, et al. Two cases of penile cancer. magnetic resonance imaging in the evaluation of tumor extension. J Urol. 1994;152:963.
17. Lont AP, Besnard AP, Gallee MP, et al. A comparison of physical examination and imaging in determining the extent of primary penile carcinoma. BJU Int. 2003;91:493.
18. Horenblas S ,van Tinteren H. Squamous cell carcinoma of the penis. IV. Prognostic factors of survival: analysis of tumor, nodes and metastasis classification system. J Urol. 1994;151:1239.
19. Horenblas S, Kroger R, Gallee MP, et al. Ultrasound in squamous cell carcinoma of the penis; a useful addition to clinical staging? A comparison of ultrasound with histopathology. Urology. 1994;43. 702.
20. Maiche AG. Computer tomography (CT) in the diagnosis and staging of cancer of the penis. Eur J Cancer. 1993;29A:779.
21. Vapnek JM, Hricak H, Carroll PR. Recent advances in imaging studies for staging of penile and urethral carcinoma. Urol Clin North Am. 1992;19:257.
22. Scardino E, Villa G, Bonomo G, et al. Magnetic resonance imaging combined with artificial erection for local staging of penile cancer. Urology. 2004;63:1158.
23. McDougal WS. Carcinoma of the penis. improved survival by early regional lymphadenectomy based on the histological grade and depth of invasion of the primary lesion. J Urol. 1995; 154:1364.
24. Bevan-Thomas R, Slaton JW, Pettaway CA. Contemporary morbidity from lymphadenectomy for penile squamous cell carcinoma. the M.D. Anderson Cancer Center Experience. J Urol. 2002;167:1638.
25. Horenblas S. Lymphadenectomy for squamous cell carcinoma of the penis. Part 1. diagnosis of lymph node metastasis. BJU Int. 2001;88:467.
26. Vassallo P, Wernecke K, Roos N, et al. Differentiation of benign from malignant superficial lymphadenopathy. the role of high-resolution US. Radiology. 1992;183:215.
27. Deurloo EE, Tanis PJ, Gilhuijs KG, et al. Reduction in the number of sentinel lymph node procedures by preoperative ultrasonography of the axilla in breast cancer. Eur J Cancer. 2003;39:1068.
28. Hall TB, Barton DP, Trott PA, et al. The role of ultrasound-guided cytology of groin lymph nodes in the management of squamous cell carcinoma of the vulva. Five-year experience in 44 patients. Clin Radiol. 2003;58:367.
29. Kuenen-Boumeester V, Menke-Pluymers M, de Kanter AY, et al. Ultrasound-guided fine needle aspiration cytology of axillary lymph nodes in breast cancer patients. A preoperative staging procedure. Eur J Cancer. 2003;39:170.
30. Rossi CR, Mocellin S, Scagnet B, et al. The role of preoperative ultrasound scan in detecting lymph node metastasis before sentinel node biopsy in melanoma patients. J Surg Oncol. 2003;83:80.

31. Kroon BK, Horenblas S, Estourgie SH, et al. How to avoid false-negative dynamic sentinel node procedures in penile carcinoma. J Urol. 2004;171:2191.
32. Harisinghani MG, Barentsz J, Hahn PF, et al. Noninvasive detection of clinically occult lymph-node metastases in prostate cancer. N Engl J Med. 2003;348:2491.
33. Wunderbaldinger P, Josephson L, Bremer C, et al. Detection of lymph node metastases by contrast-enhanced MRI in an experimental model. Magn Reson Med. 2002;47:292.
34. Tabatabaei S, Harisinghani M, McDougal WS. Regional lymph node staging using lymphotropic nanoparticle enhanced magnetic resonance imaging with ferumoxtran-10 in patients with penile cancer. J Urol. 2005;174:923.